ELSEVIER

Contents lists available at ScienceDirect

Earth and Planetary Science Letters

www.elsevier.com/locate/epsl



Rift evolution in regions of low magma input in East Africa

James D. Muirhead*, Lachlan J.M. Wright, Christopher A. Scholz

Department of Earth Sciences, Syracuse University, Syracuse, NY 13244, USA



ARTICLE INFO

Article history:
Received 9 May 2018
Received in revised form 21 October 2018
Accepted 4 November 2018
Available online xxxx
Editor: I.P. Avouac

Keywords: Lake Tanganyika magma-poor margin normal fault evolution East African Rift System Western branch continental break up

ABSTRACT

Magmatism is often invoked as critical for assisting strain focusing during continental rift development, and in driving lithospheric thinning and continental rupture. Accordingly, models of rift basin evolution in the East African Rift System (EARS) have previously focused on magma-rich basins; however, a complete understanding of how magmatism drives rift evolution requires analyses of both magma-rich and magma-poor extensional environments. We investigate a ~10-million-year history of fault development in the magma-poor Lake Tanganyika Rift of the Western branch of the EARS, utilizing reprocessed legacy and high-resolution commercial seismic reflection datasets. Unlike the magma-rich Eastern branch, faultstrain does not focus into the basin floor along the rift axis within the first \sim 10 million years of rift development. Instead, large rift-bounding faults (border faults) accommodate the majority of extensional strain (~90% of an estimated 11.5 km of extension over the 52 km-wide rift) from rift inception through to present-day rifting. The Western branch of the EARS is also characterized by crustal structure and fault geometries that differ from those observed for successfully rifted magma-poor margins (e.g., listric normal faulting with mid-crustal detachments). In the absence of voluminous magmatism, we suggest that either (1) complete continental rupture cannot be achieved in the Western branch of the EARS, or (2) continental break up in the Western branch will proceed under a model that contrasts with that invoked for both the Eastern branch and magma-poor rifted margins generally.

© 2018 Elsevier B.V. All rights reserved.

1. Introduction

The growth of upper crustal normal faults, and fault populations, plays an integral role in the development of continental rift basins (e.g., Rosendahl, 1987; Corti, 2008; Whitmarsh et al., 2001; Muirhead and Kattenhorn, 2018). These structures accommodate extensional tectonic stresses ($\sigma_{\rm V}=\sigma_1>\sigma_2>\sigma_3$) in the brittle upper crust, whereas the viscous lower crust is inferred to deform via ductile thinning and magmatism (Ebinger and Casey, 2001; Keir et al., 2006). Rift basin normal faults represent significant earthquake hazards (Biggs et al., 2010; Wauthier et al., 2015; Kolawole et al., 2017), control sediment routing patterns (Scholz et al., 1990; Ebinger and Scholz, 2012), and allow for strain focusing that leads to continental rupture and the initiation of seafloor spreading (Whitmarsh et al., 2001; Ebinger, 2005; Franke, 2013; Corti, 2009; Muirhead et al., 2016).

The East African Rift System (EARS) is an ideal site to investigate the development of fault systems as early-stage continental rifts evolve toward seafloor spreading (Ebinger and Casey, 2001; Corti, 2009; Muirhead et al., 2016; Stab et al., 2016). This > 3000 km-long continental rift is divided into Eastern and West-

* Corresponding author.

E-mail address: james.muirhead@fulbrightmail.org (J.D. Muirhead).

ern branches (Fig. 1) separated by the Archean Tanzanian Craton. Compared to the Western branch, the Eastern branch is comparatively magma-rich, with volcanic centers spatially aligned along strike over \sim 20-100 km intervals, and abundant dike-fed monogenetic volcanic cones distributed on the rift floor (Baker et al., 1971; Mohr and Wood, 1976; Biggs et al., 2009; Muirhead et al., 2015). Structural investigations of basins of different ages in Kenyan and Ethiopian sectors of the Eastern branch illustrate how fault strain is localized within basins as they evolve (Dunkelman et al., 1989; Karson and Curtis, 1989; Hayward and Ebinger, 1996; Agostini et al., 2011; Muirhead et al., 2016). Broadly, two types of fault systems accommodate extensional strain in the upper crust: (1) border faults, which bound rift segments, can be up to \sim 80-100 km-long, and accrue thousands of meters of throw; and (2) intra-rift faults, which are smaller than border faults (tens of kilometers long, with tens to hundreds of meters of throw) and form in the central, inner depressions of rift basins (Corti, 2009). During the first few million years of rifting, strain is localized along border faults accommodating asymmetric subsidence and producing basins with half-graben morphologies. These faults accrue significant amounts of throw (>1 km), and flexure of the border fault hanging wall induces extensional stresses that are accommodated via intra-rift faulting within the subsiding half-graben basin (Muirhead et al., 2016). Upper crustal strain becomes fo-

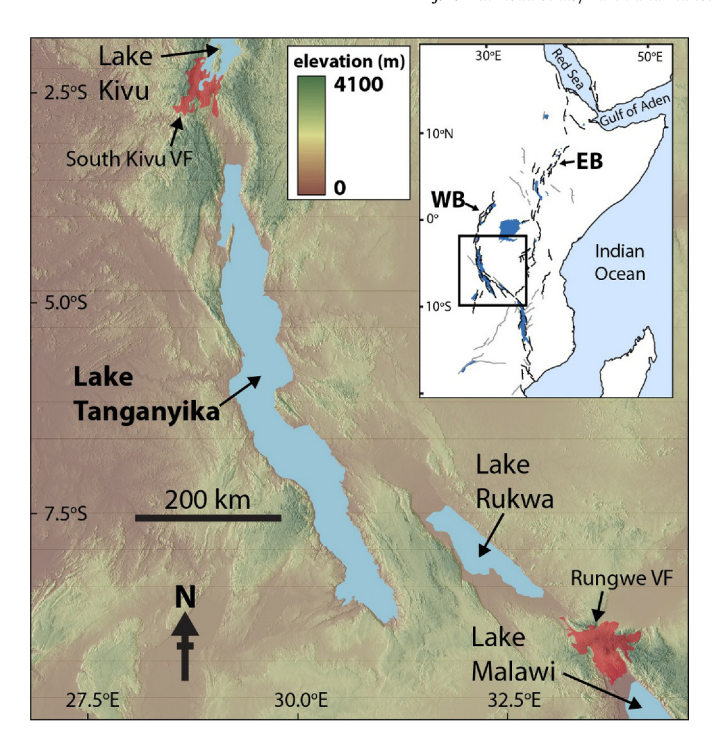


Fig. 1. Geographical location of Lake Tanganyika and surrounding rift lakes in the Western branch of the EARS. Lake waters are annotated on the 90 m SRTM dataset as light blue polygons. Also annotated are the South Kivu and Rungwe volcanic fields (VF) in red. Inset in the top right is of NE Africa showing the spatial extent of the EARS as indicated by major pre- (dark grey) and syn-rift (black) fault structures, and related lake systems (dark blue). Black box outlines the location of the main figure. The Eastern (EB) and Western branches (WB) are also annotated. (For interpretation of the colors in the figure(s), the reader is referred to the web version of this article.)

cused within the intra-rift fault system after 3 to 7 million years of rifting, with an accompanying reduction in the rate of border fault slip (Muirhead et al., 2016). This transition to intra-rift faulting in the 3–7 Ma Natron and Magadi basins (Kenya–Tanzania) coincides with the emplacement of lower crustal magmas below the center of the basin and release of magmatic fluids along deeply penetrating faults (Lee et al., 2016; Muirhead et al., 2016; Lee et al., 2017; Plasman et al., 2017; Weinstein et al., 2017). Overall, these studies suggest that strain focusing within fault populations of the Eastern branch is assisted by the mechanical and thermal effects of magma intrusion (Karson and Curtis, 1989; Buck, 2004; Beutel et al., 2010; Bialas et al., 2010), as well as fluid-driven weakening (Muirhead et al., 2016; Lee et al., 2017; Weinstein et al., 2017)

With the exception of magma-rich transfer zones (also called accommodation zones; e.g., Rosendahl, 1987; Hayward and Ebinger, 1996) that develop in the linkage areas between segmented rift basins (e.g., Virunga Proince, north Kivu; Corti et al., 2004; Wauthier et al., 2013), rift development in the Western branch is observed to occur in the absence of magmatism (O'Donnell et al., 2013; Shillington et al., 2016; Accardo et al., 2017), or significantly lower volumes of intruded magma (O'Donnell et al., 2015; Hodgson et al., 2017). Instead of magmatic weakening influencing the development of fault systems, preexisting structures are thought to play a critical role in strain localization processes (Daly et al., 1989; Kilembe and Rosendahl, 1992; Wheeler and Karson, 1994; Klerkx et al., 1998; McCartney and Scholz, 2016). Although the general geometric configuration of border fault systems is well constrained for many Western branch basins (e.g., Rosendahl, 1987; Morley, 1988), very few studies have investigated the temporal development of these fault systems in great detail. To address this question, McCartney and Scholz (2016) recently applied syndepositional fault analyses interpreted from 2-D reflection seismic data of the \sim 6 Ma Malawi Rift. This study revealed a 1.3 Myr (million year) history of intra-rift faulting in this basin, and concluded that intra-rift faults were established early in basin's history (sometime within the first 5 million years) and during this time were active synchronously with the border fault system, much like that observed for the Eastern branch (Agostini et al., 2011; Muirhead et al., 2016). However, the geochronological constraints in McCartney and Scholz (2016) did not permit an investigation of older fault displacements (2 to 6 Ma) in this \sim 6 Myr-old rift, and the timing of fault initiation and their evolving role in strain accommodation as the basin developed is unresolved.

It is therefore still unknown if and when intra-rift faulting becomes the dominant mode of upper crustal strain accommodation in Western branch rifts, which appear to be initiated with a very low magma supply (O'Donnell et al., 2013, 2015). Basin development models for the Eastern branch of the EARS suggest that the transition to intra-rift dominated strain accommodation is a critical process during rift evolution to seafloor spreading (Ebinger, 2005; Corti, 2009; Muirhead et al., 2016). In older (>10 Ma) and presumably more evolved basins in the Main Ethiopian Rift, these intra-rift fault systems represent the upper crustal expression of magmatic segments (refer to Ebinger and Casey, 2001; Keir et al., 2006), which are also inferred to be nascent spreading ridges (Ebinger, 2005; Corti, 2009). Some authors advocate that the development of magmatic segments in the Eastern branch occurs in response to decompression melting below the rift center from lithospheric thinning during intra-rift fault development (Corti, 2008); hence, without strain focusing into intra-rift faults in the basin center and its related magmatism, it may be that complete continental rupture cannot occur in thick lithosphere in East Africa (Buck, 2004; Bialas et al., 2010).

Here we address the role of intra-rift faulting over the course of rift evolution in the Western branch, through a seismic reflection data analysis of the ~10 Ma Lake Tanganyika Rift (Cohen et al., 1993). The distribution and orientations of rift faults are compared with inherited basement fabrics (e.g., Precambrian shear zones of Choubert and Faure-Muret (1968)) observed along uplifted rift flanks. Syn-depositional fault analyses on intra-rift faults from newly reprocessed and commercial seismic reflection data reveal the timing of fault development, and how fault throw has accumulated on individual faults through time, as documented by displacements observed on horizons bounding successive intervals of the syn-rift sequence. These data provide new insights into how strain localization proceeds and evolves in an area of reduced magmatism in the Western branch, thereby testing the importance of magma for assisting continental rift evolution and breakup. Results and observations from our study region are then compared with successfully rifted magma-poor margins to examine the efficacy of break up processes in the Western branch.

2. Regional geology

The Lake Tanganyika Rift is a mid- to late-Miocene, multisegment rift basin situated in the relatively magma-poor Western branch of the EARS (Rosendahl, 1987; Morley, 1988) (Fig. 1). The surface of the modern-day lake has an elevation of 767 m above mean sea level (amsl), and rift-associated topography on border fault footwall uplifts is as much as 3500 m amsl. Age estimates based on short-term sediment accumulation rates from core sampling and depth-to-basement estimates support rifting initiation at Lake Tanganyika at 9–12 Ma (Cohen et al., 1993). An earlier phase of rifting at ~25 Ma is hypothesized for the neighboring Rukwa Rift, which is situated ~100 km east of southern Lake Tanganyika (Roberts et al., 2012). Extension and related basin subsidence is driven primarily through displacements along

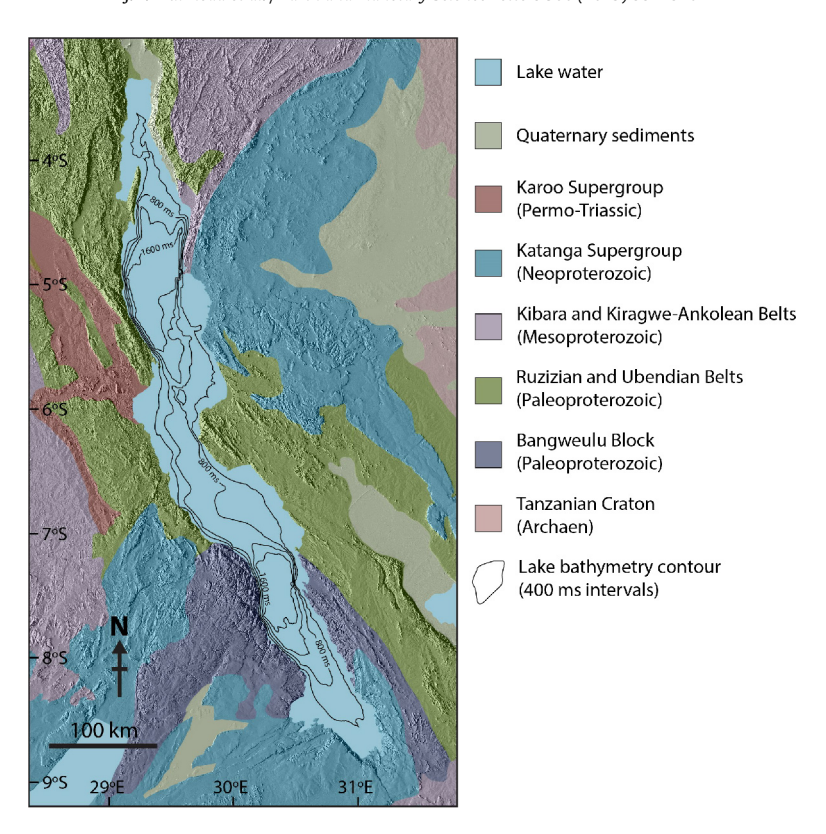


Fig. 2. Broad distribution of major geological units in the Lake Tanganyika region, modified from Choubert and Faure-Muret (1968) and annotated on the 90 m SRTM DEM. Within the lake are bathymetric contours derived from multichannel seismic data (400 ms TWTT contour spacing).

major rift-bounding faults (Morley, 1988) to produce the world's second deepest lake, with a maximum depth of \sim 1450 m. Nine border faults are observed across the lake and define a series of rift segments that are kinematically linked by transfer (or accommodation) zones (Rosendahl, 1987; Morley, 1988). Basin segments commonly exhibit the half-graben morphologies characteristic of the EARS, although a few segments form as full-grabens (Morley, 1988). Extension directions are restricted to sparse GPS measurements and focal mechanism inversions (Delvaux and Barth, 2010; Saria et al., 2014), which support an E–W- to ESE–WNW-trending least compressive stress in the northern half of the lake, and NE–SW-trending least compressive stress in the south (Delvaux and Barth, 2010).

Surficial deposits adjacent to Lake Tanganyika show no significant evidence of volcanism during rifting, other than thin (<1 cm) Holocene tephras associated with Rungwe volcanic province eruptions, and volcanic centers across the Tanganyika-Malawi Rift sector are >500 km apart (Fig. 1). Accordingly, many authors suggest the Lake Tanganyika Rift, and Western branch generally, is "amagmatic" or magma-poor (Kilembe and Rosendahl, 1992; Muirhead et al., 2015; Accardo et al., 2017). Consistent with these assertions, geophysical evidence for melt bodies in the upper mantle is absent in the Lake Tanganyika region (O'Donnell et al., 2013, 2015). However, V_D/V_s ratios suggest that magma and/or fluids potentially reside in the lower crust in southern Lake Tanganyika, primarily below the uplifted eastern rift flank in the transfer zone between the Rukwa Rift, with potential lower crustal melt also below the Manda graben (Hodgson et al., 2017). Similarly, sub-lacustrine hydrothermal vents documented in north Lake Tanganyika exhibit $\delta^{13}C$ values of dissolved carbon dioxide ranging -3.8 to -9.1% (Botz and Stoffers, 1993), which are within the range of isotopic values of magmatic volatiles measured in the Kenya Rift (Lee et al., 2017). The volumes of intruded magmas situated below Lake Tanganyika are unresolved, but are interpreted to be a fraction of those intruded in basins in the

Eastern branch, which exhibit abundant geophysical, geological, and geochemical evidence for lower crustal magmatic modification (Baker et al., 1971; Mechie et al., 1994; Ebinger and Casey, 2001; Keir et al., 2009), widespread volcanism (Baker et al., 1971), active intrusion (Wright et al., 2006; Calais et al., 2008; Biggs et al., 2011; Weinstein et al., 2017), and widespread magmatic CO₂ degassing (Hunt et al., 2017; Lee et al., 2017).

Syn-rift sedimentary sections of the Lake Tanganyika Rift are rarely exposed onshore (Tiercelin et al., 1992), although outcrops of crystalline bedrock are commonly observed on the coastline and outward into the surrounding rift flanks (Fig. 2). The Lake Tanganyika Rift occurs preferentially within Proterozoic and early Phanerozoic mobile belt rocks (typically high-grade metamorphic rocks) positioned on the periphery of the Archean Tanzania craton (primarily plutonic rock). Lithosphere in these mobile belts is thought to be weaker than the surrounding craton, and hence extensional deformation has localized along preexisting shear zones within these mobile belts (Daly et al., 1989; Klerkx et al., 1998). Little is known of the thick syn-rift sequence of the Lake Tanganyika Rift, primarily due to a lack of deep drill cores in the sedimentary section. Sediment cores extend no deeper than \sim 10 m, providing a \sim 30-100 kyr record of sedimentation (Cohen et al., 1993; Scholz et al., 2003). Legacy 2-D reflection seismic data (Rosendahl et al., 1988) acquired in a reconnaissance grid over Lake Tanganyika were originally interpreted to show two major seismic stratigraphic units in the lower and upper parts of the syn-rift sequence; these interpretations are further subdivided in the current study using recently acquired commercial seismic reflection data (outlined in Supplemental Text). The lower part of the syn-rift sequence (Magara Sequence: Rosendahl et al., 1988; Macgregor, 2015) typically comprises lower amplitude, chaotic discontinuous reflections overlain by continuous, high-amplitude, low-frequency reflectors. The age of this unit is thought to range from middle Miocene to early Pliocene (Cohen et al., 1993). The

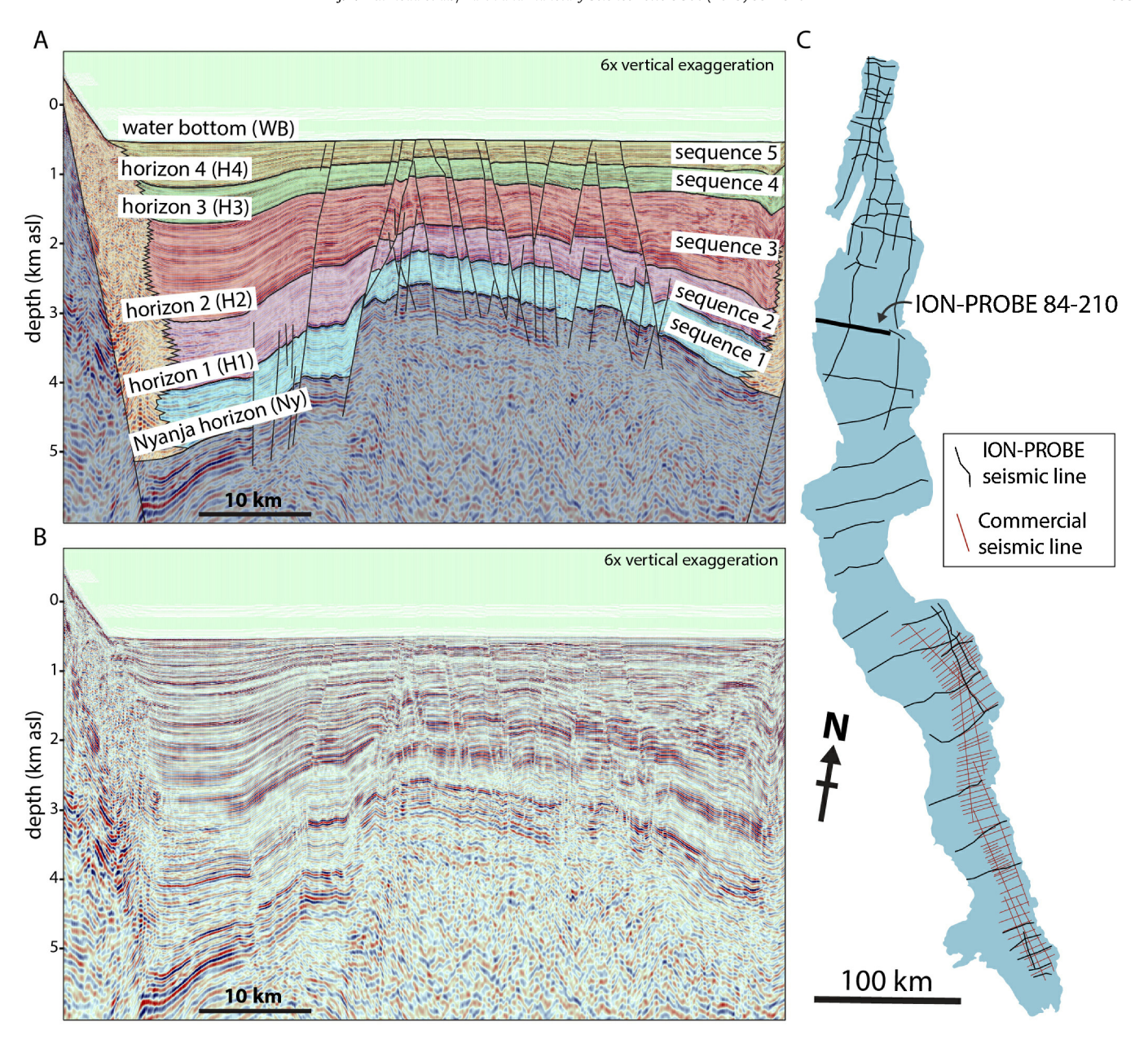


Fig. 3. Interpretation of seismic profile line ION-PROBE 84-210. (A) Interpreted depth section showing the key horizons and major sequences in the syn-rift section, and major normal faults. Acoustic basement is colored dark greyish blue, and border fault fan delta/talus deposits are colored peach. (B) Un-interpreted depth seismic section. Note the characteristic attenuation of the seismic signal below the Nyanja Horizon. (C) Inset showing the location of ION-PROBE line 84-210 and the extent of seismic reflection data throughout Lake Tanganyika used in this study. Black lines and red lines show the line distribution the ION-PROBE and commercial seismic datasets.

upper half of the syn-rift sequence (Kigoma Sequence: Rosendahl et al., 1988; Macgregor, 2015) is typically composed of continuous, high-amplitude, high-frequency reflectors. The possible age range of this unit is early Pliocene to Holocene, based on ages from Cohen et al. (1993).

3. Methods

3.1. Reflection seismic datasets

Our study utilizes over \sim 1900 km of reprocessed legacy Project PROBE data acquired in Lake Tanganyika (Rosendahl et al., 1988) (Fig. 3). These 24-fold reflection seismic data have an average spacing of 18 km between lines and were acquired using a 140 cubic inch single air gun and a 48-channel hydrophone streamer, with a maximum offset of 1450 m. The legacy PROBE dataset (for original seismic profiles, refer to Rosendahl et al., 1988 and Morley,

1988) was reprocessed in 2016 by ION Geophysical using modern algorithms, and pre-stack depth migrated, and is referred to herein as the ION-PROBE dataset. A detailed summary of processing routines is provided in the Supplemental Information. In addition to the ION-PROBE data, our analyses are supplemented by 2D commercial multichannel reflection seismic data collected in 2012 for the Tanzania Petroleum Development Corporation in the southeastern part of the lake. The 60-fold commercial data are broad band (\sim 5-75 Hz), and were acquired using a 3 km-long streamer and a 500 cubic inch air gun array. These data have a higher resolution and higher spatial density (typical line-spacing of \sim 3 km) than the ION-PROBE data, but are restricted to <20% of the lake, whereas the ION-PROBE data are distributed across the entire basin (Fig. 3). The two datasets are thus complementary, where the commercial data provide detailed information on the stratigraphic framework (see Supplemental Text).

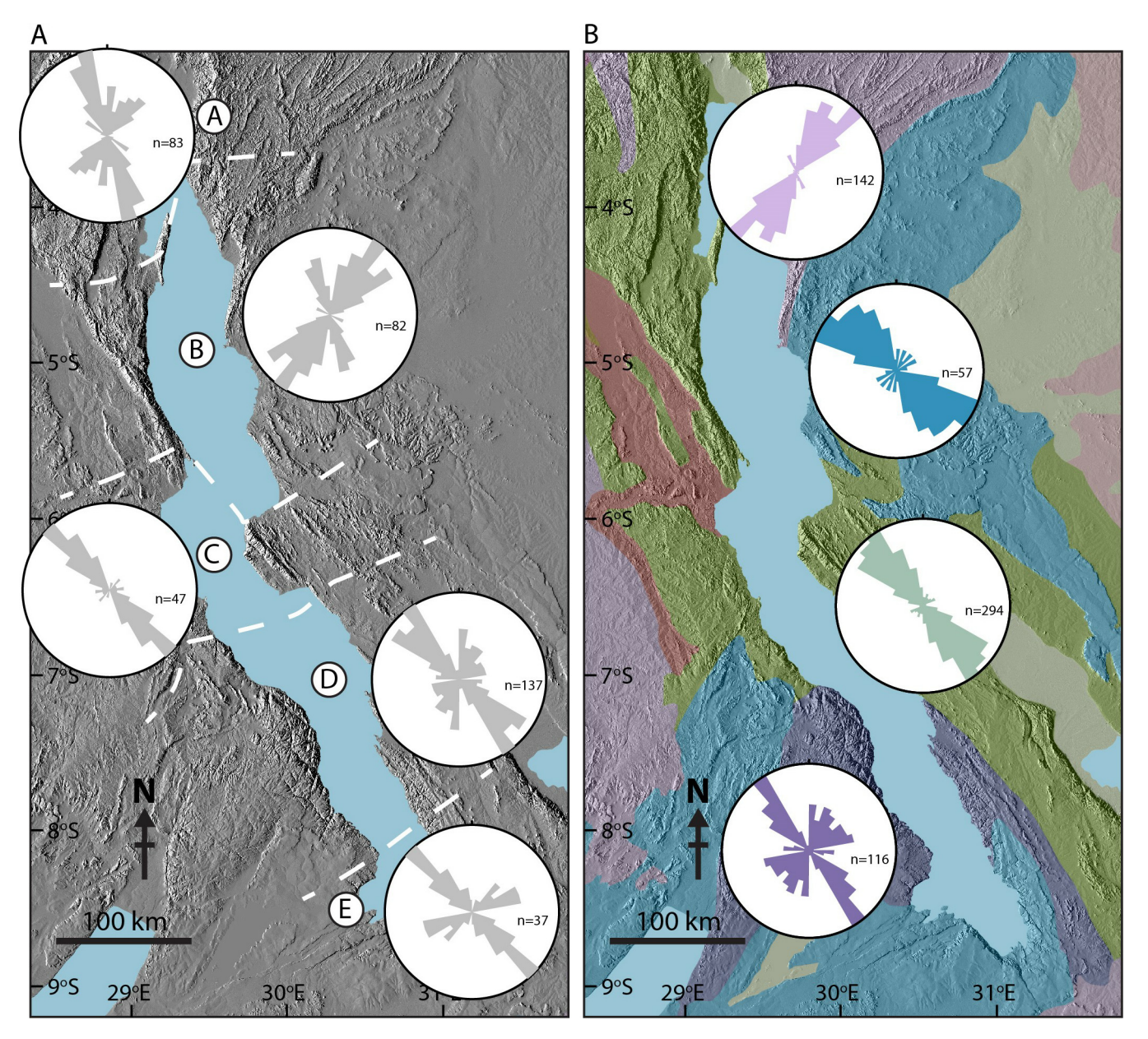


Fig. 4. Results of lineament analyses in Precambrian basement on the flanks of the Lake Tanganyika Rift annotated on the 90 m SRTM dataset. (A) Rose diagrams showing the trends of major (lengths >10 km) pre-existing lineaments within the various structural provinces. From north to south these provinces are the (a) Ruzizi, (b) Kigoma, (c) Kalemie, (d) Marungu, and (e) Mpulungu provinces. (B) Rose diagrams showing the trends of major (lengths >10 km) pre-existing lineaments within different basement terranes (key provided in Fig. 2). The pink, blue, green, and purple rose diagrams correspond to lineaments in the Kiragwe–Ankole Belt, Katanga Supergroup, Ruzizian–Ubendian Belt, and Bangweulu Block, respectively.

3.2. Mapping faults and preexisting structures from remote sensing datasets

Neogene faults and preexisting Precambrian structures around the margins of Lake Tanganyika were interpreted, mapped, and analyzed in the study region using the 30 m SRTM (both DEM data and hillshades), with the aid of existing maps (e.g., Choubert and Faure-Muret, 1968) (Fig. 4). Lineaments with lengths >10 km and exhibiting observable surficial scarps (minimum relief of 30 m) were interpreted as fault segments. Pre-existing basement structures (e.g., fractures, shear zones) were extracted from the geological map of Choubert and Faure-Muret (1968), and compared with interpreted lineaments from the 30 m SRTM data. These features are located in the Kibara–Karagwe–Ankolean and Ruzizi–Ubendien belts, Katanga Supergroup, and Bangweulu Block. The criteria for identifying these features are discussed in the Supplemental Text.

3.3. Seismic stratigraphy of Lake Tanganyika

Our interpretation of syn-rift sequences is based on the seismic stratigraphy interpreted from the commercial dataset (see also Supplemental Text). Six major depositional sequences are observed within syn-rift sediments of the Marungu and Mpulungu provinces in southeast Lake Tanganyika. The sequences are interpreted based on stratal relationships of the bounding stratigraphic surfaces, such as erosional truncation, onlap, and downlap, and the acoustic character of the stratigraphic units. Following the interpretation of Rosendahl et al. (1988), the base of the syn-rift sequence is defined by a distinct low-frequency, high-amplitude seismic reflector, termed the Nyanja Event. This horizon was previously interpreted as the contact between rift basin sediments and crystalline basement (e.g., Rosendahl et al., 1988).

3.4. Reflection seismic analyses of fault system development

Faults within the Lake Tanganyika syn-rift sequence were mapped using ION-PROBE and commercial reflection seismic data. Baudon and Cartwright (2008) show that errors in throw values for faults analyzed in 2D reflection seismic are approximately equal to the sample rate of the data. Therefore, we expect that faults with throws >2 ms can be theoretically identified using the ION-PROBE and commercial seismic data, respectively (based on the sampling rate of the data). A regional profile along the Kigoma basin was restored and balanced (i.e., conserving area) using the depth converted ION-PROBE lines 84-210 and 83-38, as well as ASTER DEM data, using the Lithotect structural restoration software (see Supplemental Information), to provide a revised estimate of total horizontal stretching in the Lake Tanganyika Rift. This approach of using seismic profile lines is inherently 2D; however, our study is primarily focused on the history of rifting observed up the syn-rift sequence, and seismic sections within the deeply subsided Kigoma basin represent the ideal candidate sections for such an analysis (discussed further in Section 3.5).

3.5. Analysis of syn-depositional faulting

We performed a syn-depositional (growth) fault analysis in the Kigoma basin from a depth-converted section of seismic line ION PROBE 84-210 (see also Supplemental Text). The Kigoma basin represents one of the most deeply subsided and oldest basins in the multi-segment Lake Tanganyika Rift system (Cohen et al., 1993) (Figs. 2 and 3), and therefore provides a longer history of fault development compared to shallower, thinner, and possibly younger basins in the south and north. With water bottom depths >1000 m, seismic facies over much of the basin show exceptional reflection continuity compared to other seismic lines (see Rosendahl et al., 1988). This supports the interpretation that the thick sedimentary pile (>5 km in places) was fully subaqueous over its history, representing a complete sedimentary sequence with high temporal continuity, and uninterrupted by erosional events during lake low-stands (Scholz et al., 2007). For example, in the middle to late Pleistocene, lake levels were at times more than 600 m lower than the present level (Scholz and Rosendahl, 1988). The main seismic profile line through the center of the Kigoma basin (ION-PROBE 84-210) also trends 095° and approximately parallel to the regional extension direction from analysis of earthquake focal mechanism and GPS data (Delvaux and Barth, 2010; Saria et al., 2014). The analyzed seismic section is therefore optimally oriented (parallel to fault dip direction) with respect to the ~N-S-striking faults in the northern half of Lake Tanganyika Rift.

3.5.1. T-z plots

Throw (T) versus depth (z) plots are commonly used to study fault evolution in both 3D and 2D reflection seismic data in sedimentary basins worldwide, including the Eastern Mediterranean (e.g., Baudon and Cartwright, 2008), the North Sea (e.g., Duffy et al., 2015), the Suez Rift (e.g., Jackson and Rotevatn, 2013), Gulf Coast (Cartwright et al., 1998), and EARS (McCartney and Scholz, 2016). The method has also been applied in paleoseismic analyses of normal fault systems onshore, and when combined with age constraints, can provide time-averaged slip-rates (Berryman et al., 2008). For syn-depositional (growth) faults in sedimentary rift basins, throw is gradually accumulated during deposition of syn-rift sediments. Depending on the rate of sedimentation, the fault scarp developing at the surface will be completely covered in sediment, so that the amount of observable throw at the surface approaches zero, whereas the total throw accumulated over the lifetime of the fault can only be confidently measured along the basement horizon (base of the syn-rift sequence). Plotting stratigraphic throw vs. depth (or throw vs. time) on syn-depositional faults thus reveals temporal (or depth) variations in throw, which can be used to estimate the amount of throw accumulated along a fault during different depositional time periods (e.g., Berryman et al., 2008). Here, we calculate stratigraphic throw (T) on horizons in the depth-converted sections by measuring the vertical separation, in meters, between the hanging wall and footwall cutoffs for the horizon (Eq. (1)):

$$T = z_{\rm H} - z_{\rm F} \tag{1}$$

where z_H is the depth of the hanging wall cutoff and z_F is the footwall cutoff depth for the same horizon. The depth (z) in the T-z plot is the depth of the midpoint between the hanging wall and footwall cutoffs (Eq. (2)):

$$z = z_{\rm F} - 0.5T \tag{2}$$

Finally, the total throw accumulated during each sequence, bounded by the 5 major horizons identified in the current study (Fig. 3), is estimated using the following (Eq. (3)):

$$T_{\rm S} = T_{\rm L} - T_{\rm U} \tag{3}$$

where T_S is the throw accumulated during the sequence of interest, and T_L and T_U are the measured throw on the lower and upper horizons, respectively, of the sequence.

4. Structural data

4.1. Pre-existing structures

Remote sensing analyses of Precambrian basement fabrics in our study area are in good agreement with the regional geological map of Choubert and Faure-Muret (1968) (Fig. 4). Overall, these data reveal systematic variations in inherited fabrics between different basement terranes. The dominant basement fabric in the Lake Tanganyika Rift region trends NW-SE. Within the Bangweulu Block, near the SW sector of the lake, this NW-SEtrending fabric is present, although there is also a weak NE-SWtrend (Fig. 4). Fabrics within Ruzizian-Ubendien Belt rocks trend NW-SE. Similar NW-trending fabrics are observed on the western margin of the lake in Permo-Triassic Karoo rocks, and follow the trend of inferred Karoo-age faults (Klerx et al., 1998). Near the center of the Lake Tanganyika Rift, and east of the lake, we observe NW-SE-trending lineaments in the Katanga Supergroup. In the north, within the Kiragwe-Ankole Belt, basement fabrics trend NW-SE.

4.2. Rift faults

4.2.1. Comparison with previous fault maps

Original fault mapping within the offshore syn-rift sedimentary section by Rosendahl (1987) resulted in nine interpreted border faults bounding Lake Tanganyika. Border fault traces were originally interpreted to form idealized arcuate shapes in map-view (Rosendahl, 1987) in accordance with preconceived models of rift architecture, although later interpretations (e.g., Morley, 1988) favored straight fault traces in plan-view and between nine and twelve border faults. The strict lineament identification criteria applied in the current study (see Supplemental Text) results in linear fault traces (bother border and intra-rift faults) similar to Morley (1988), and a significant reduction in the number of transverse faults (i.e., structures striking oblique to the dominant fault pattern and lake shoreline) (Fig. 5). This revised interpretation contrasts

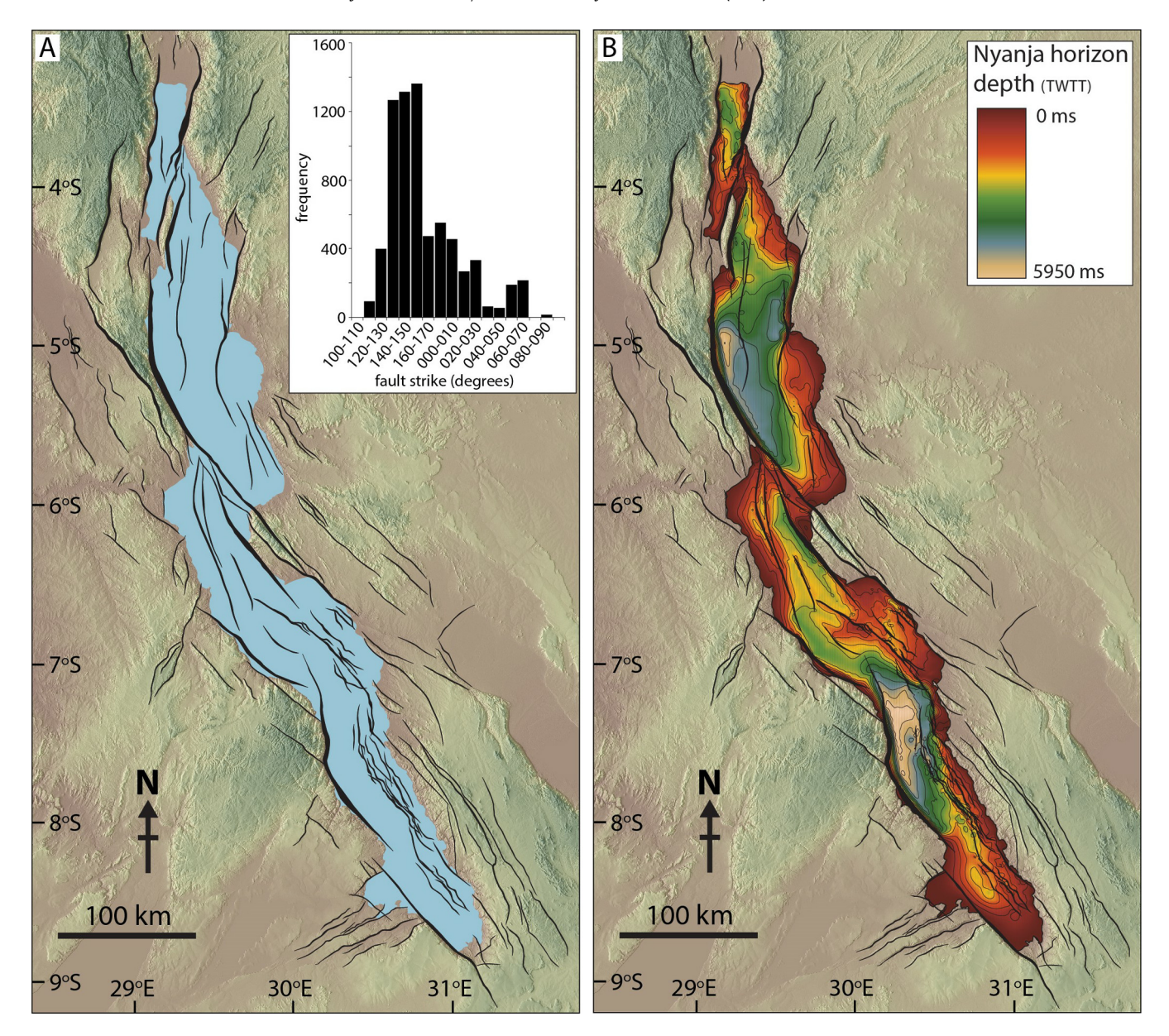


Fig. 5. Structure of the Lake Tanganyika Rift annotated on the 90 m SRTM dataset. (A) Distribution of faulting with respect to the rift lake (blue polygon). Histogram in the top right is of length-weighted fault trends for faults within and up to 100 km outside the lake. (B) Structure contour plot of Lake Tanganyika in two-way travel time (TWTT). Contour map represents the depth to the base of the syn-rift section (Nyanja Horizon) from the lake surface.

with earlier work of Rosendahl et al. (1992) (Fig. 6). However, the interpreted fault traces, and dominantly rift-parallel fabric, are geometrically similar to subaerially exposed fault systems in rift basins in Kenya and Ethiopia (e.g., Agostini et al., 2009; Muirhead et al., 2015, 2016), and faults within the syn-rift sequence strike subparallel to faults observed in the 30 m SRTM data outside of the lake. As such, we suggest the combined use of ION PROBE and 30 m SRTM data provides the most accurate interpretation of fault systems in Lake Tanganyika to date.

4.2.2. Regional fault trends

We identify nine border faults in the syn-rift sequence of Lake Tanganyika, and 55 smaller, intra-rift faults meeting our mapping criteria, as well as 96 faults in basement rocks outside of the lake. The length-weighted histogram plot of fault trends in Fig. 5 reveals dominantly NW-trending faults in the Lake Tanganyika Rift. Additionally, NE-trending and N- to NNE-trending fault sets are observed in several localities (Fig. 7).

Fault data were subdivided based on the 5 structural provinces of Rosendahl et al. (1988), the boundaries of which have been slightly adjusted based on the revised distribution of border faults in the current study (Fig. 7). Fault trends in the Lake Tanganyika Rift vary from south to north between the different structural provinces, with up to three fault populations in each province based on the grouping of fault data (Fig. 7). The southernmost province, the Mpulungu Province, exhibits a primary NW-trending fault population with a subsidiary NE-trending fault set. The Marungu Province is dominated by NW-tending faults. A primary NW-trending fault set is also observed in the Kalemie Province, with minor NE-tending faults. Farther north, in the Kigoma Province, N- to NNE-trending faults are more prevalent than in the south, although NW-trending faults are observed. In the northernmost province, the Ruzizi Province, faults are almost exclusively grouped into N- to NNE-trends. The strike of the primary fault fabric rotates overall in a clockwise direction from south to north, from a dominantly NW-orientation in the south to a NNE-orientation in the north.

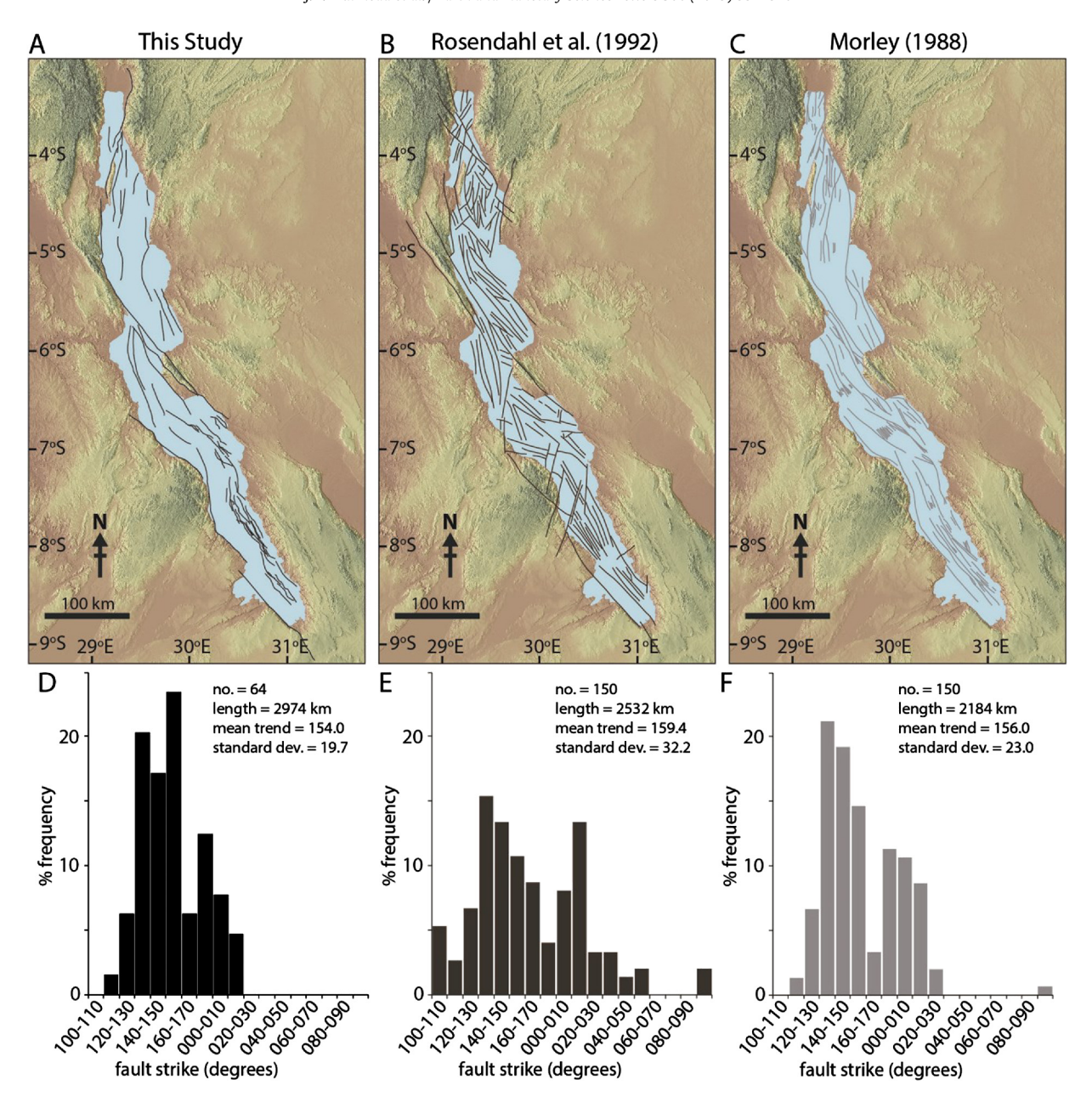


Fig. 6. Comparison of fault trends for mapped faults within Lake Tanganyika between the current and previous studies. Fault maps (a)–(c) are annotated on the 90 m SRTM DEM. The % frequency histograms correspond to faults trends from (d) this study, (e) Rosendahl et al. (1988), and (f) Morley (1988). To ensure consistency between datasets, only faults that occur on the lake edges and/or those inferred to dissect the syn-rift sequence were analyzed. Therefore, the off-rift structures presented in Fig. 8 are not included on the histogram plot in (d).

4.3. History of faulting and extension in the Kigoma basin

Structural restorations (Fig. 8) of the 52 km-wide Kigoma basin provide a β -factor of 1.283, or 28.3% crustal extension. This extension is primarily accommodated along the eastern and western border faults, which exhibit cumulative heaves of \sim 10,000 m, accounting for \sim 87% of the total horizontal extension in the basin (Fig. 8). Crustal thinning values estimated in our study are consistent with crustal thinning estimates from receiver function analyses in southern Lake Tanganyika (β -factor up to 1.33; Hodgson et al., 2017). However, our estimate of 11.5 km of crustal extension is higher than previous estimates for basins along the Western branch, which typically range 3 to 10 km (Ebinger et al., 1991). It is also greater than previous extension estimates by Morley (1988) in Lake Tanganyika of 4–5 km based on analyses of legacy reflection seismic data (e.g., Project PROBE), although Morley (1988) did

not consider rift flank uplifts in border fault footwalls outside the extent of the seismic profiles (Fig. 8).

Fault throw histories of the intra-rift faults are inferred from T–z plots in the Kigoma basin (Fig. 9; Table 1). The Nyanja event is displaced by 80% of the intra-rift faults, with all faults exhibiting increasing throw values that tend toward zero at the surface, consistent with syn-depositional faulting. By contrast, 20% of faults in the syn-rift sequence exhibit throw vs. depth values consistent with isolated faults (for terminology, see Jackson and Rotevatn, 2013), where faults are not basement-involved or where the greatest throw along the fault occurs in shallower parts of the syn-rift sequence above the basement horizon. These were not considered in our final T–z analysis, nor in our estimates of fault slip during deposition of each sequence. Overall, throws along isolated intra-rift faults in the Kigoma basin amount to a total of 144 m, representing \sim 5% of the total intra-rift fault displacement (3180 m

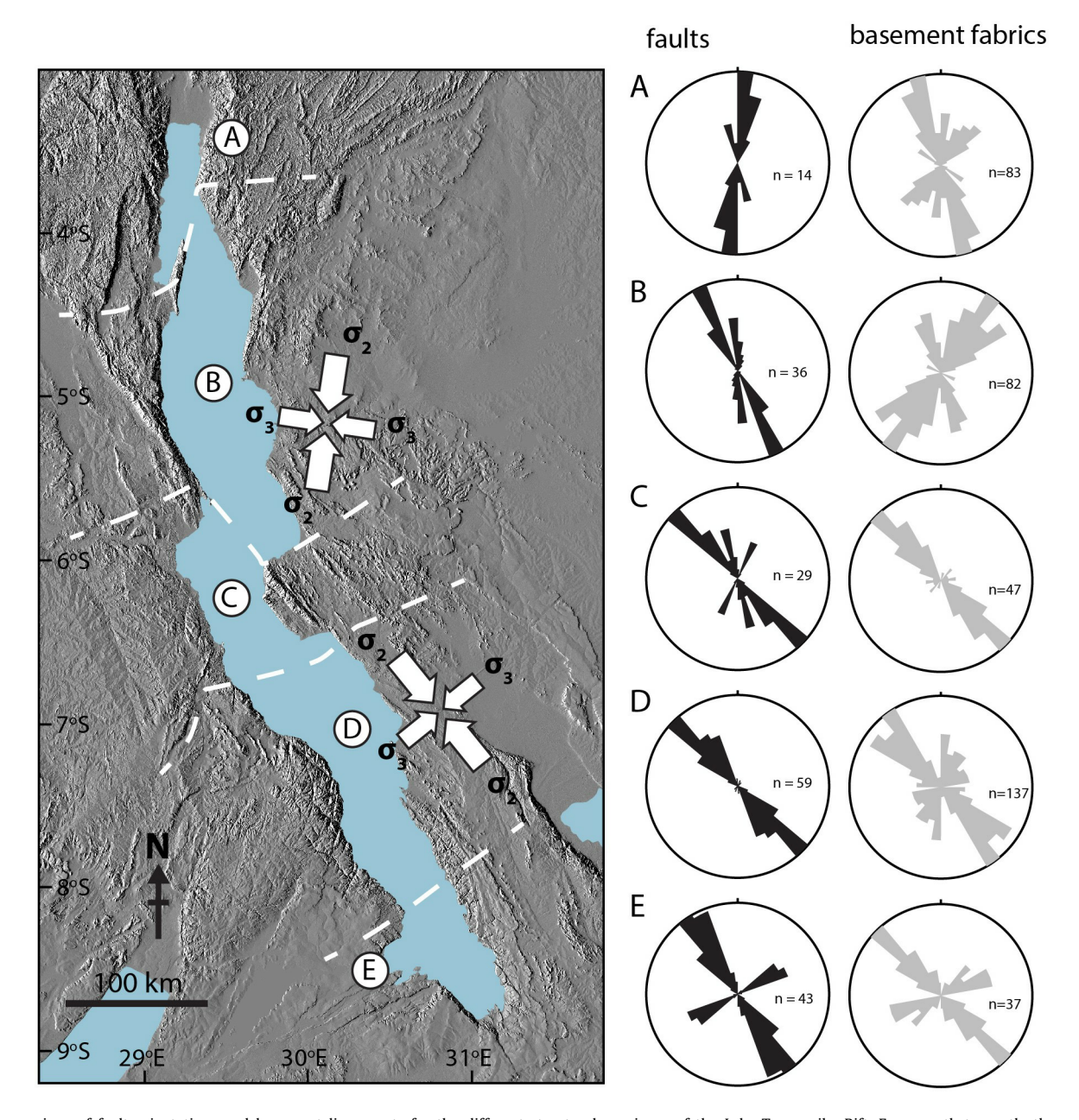


Fig. 7. Comparison of fault orientations and basement lineaments for the different structural provinces of the Lake Tanganyika Rift. From north to south, these provinces include the (a) Ruzizi, (b) Kigoma, (c) Kalemie, (d) Marungu, and (e) Mpulungu provinces. Black rose diagrams show the trends of normal faults, whereas the grey rose plots are the trends of basement lineaments (presented also Fig. 4a). Large and small white arrows represent the orientations of the least (σ_3) and intermediate (σ_2) compressive stresses from Delvaux and Barth (2010) for northern and southern portions of Lake Tanganyika.

cumulative throw); therefore, discarding these second-order structures from our analyses has a negligible impact on the final results.

Syn-depositional fault analyses provide insights into the broad timing of fault initiation (Fig. 9; Table 1). Our analyses suggest that activity on all the resolved syn-depositional faults had initiated by the end of Sequence 3 in the Pliocene. Most of these faults activated early in the basin's history, with 64% initiating during Sequence 1, and 32% during Sequence 2.

Throw on these intra-rift faults decreases up-sequence, and thus over the course of basin development (Fig. 9; Table 1), consistent with growth faulting. Within Sequences 1 and 2 (middle Miocene to early Pliocene), intra-rift faults have cumulative throws of 2265 m. By contrast, during Sequence 3 to 5 (early Pliocene to present) intra-rift faults accumulated 915 m of throw. These results illustrate that $\sim\!70\%$ of the cumulative intra-rift fault strain (3180 m of throw) occurred during the earliest stages of

rifting, suggesting that intra-rift fault activity has decreased over the course of rifting. These conclusions are verified by calculated β -factors for the intra-rift faults in our structural reconstructions. In the intra-rift fault population, a β -factor of 1.021 is estimated for intra-rift faults during deposition of Sequences 1 to 2 (60% of intra-rift extension), compared to β -factor of 1.014 during Sequences 3–5 for the \sim 52 km-wide zone of rifting.

5. Discussion

5.1. Controls on fault orientations

Revised fault mapping of the Lake Tanganyika Rift from both remote-sensing and reflection seismic datasets reveals systematic variations in fault orientations from south to north along the rift. Broadly, the rift has localized within Precambrian mobile belt

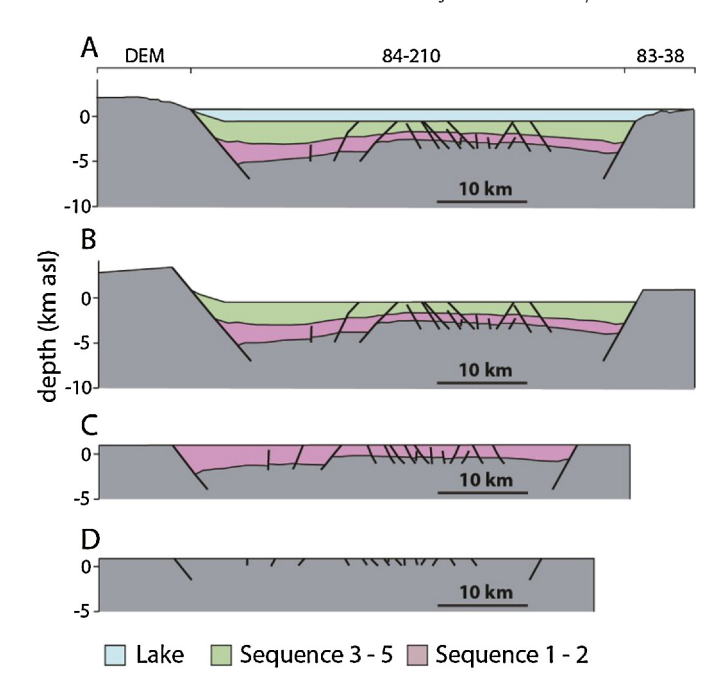


Fig. 8. Balanced (A) and restored (B)-(D) regional profiles across Lake Tanganyika constructed from ION-PROBE 84-210, ION-PROBE 83-38, and ASTER data (1:1 vertical to horizontal scale). Exact location of the regional profile line is presented in Fig. S4. Note that the complete removal of lake water and restoration of each sequence to the regional pin represents the standard simplified approach for all reconstruction studies; however, some volume of lake water is expected to be present at all stages, and border fault displacements depicted between stages (B) and (C) represent maximum values. (B) Regional profile after removal of the water column and decompaction. The topographic profile of the border fault footwall was reconstructed to a pre-erosion state by fitting a line to the mean elevation profile estimated from eight separate topographic profiles on the rift flanks of the Kigoma basin (Supplemental Fig. S4). (C) Regional profile after restoration and decompaction of sequence 1-2. The reconstruction method minimizes topography on the uplifted rift flanks, and therefore the observed border fault configuration during this restored stage does not represent the true rift topography at the end of deposition of Sequences 1 and 2. (D) Restoration of basement to the regional pinpoints. A detailed description of the methods and results are provided in the Supplemental Text. Profile location provided in Supplemental Fig. S3.

rocks, rather than Archean cratonic lithosphere (Daly et al., 1989; Fig. 2). In places, fault patterns mimic the inherited fabric (Fig. 7). Broadly, the NW-striking faults trend parallel with preexisting basement fabrics in the Katanga Supergroup, Katanga Supergroup, Ruzizian–Ubendian Belt, and Bangweulu Block, as well as Karoo rift structures (Klerx et al., 1998). These observations highlight the possible influence of inherited crustal weaknesses on fault orientations and strain localization within the rift (Versfelt and Rosendahl, 1989; Klerkx et al., 1998).

In the Kigoma and Ruzizi Provinces, however, the N- to NNE-trending faults strike oblique (i.e., >20°) to the dominant trends of preexisting lineaments in the Precambrian terranes, which are NNW-SSE and NE-SW in the Ruzizi and Kigoma Provinces, respectively. Instead, these N- to NNE-trending faults are oriented normal to the regional extension direction inferred from GPS-based modeling (Saria et al., 2014) and to the minimum horizontal stress direction from inversion of focal mechanism data (Delvaux and Barth, 2010) (Fig. 7). These optimally-oriented faults (i.e., faults striking normal to the minimum horizontal stress) may have instead activated intact rock, rather than utilizing the pre-existing grain observed in our lineament analyses.

Data from Delvaux and Barth (2010) also support local stress rotations in the central and southern parts of Lake Tanganyika, such that the least compressive stress is oriented normal to the many NW–SE-trending faults (Fig. 7). The local stress field may therefore provide the dominant control on the observed normal

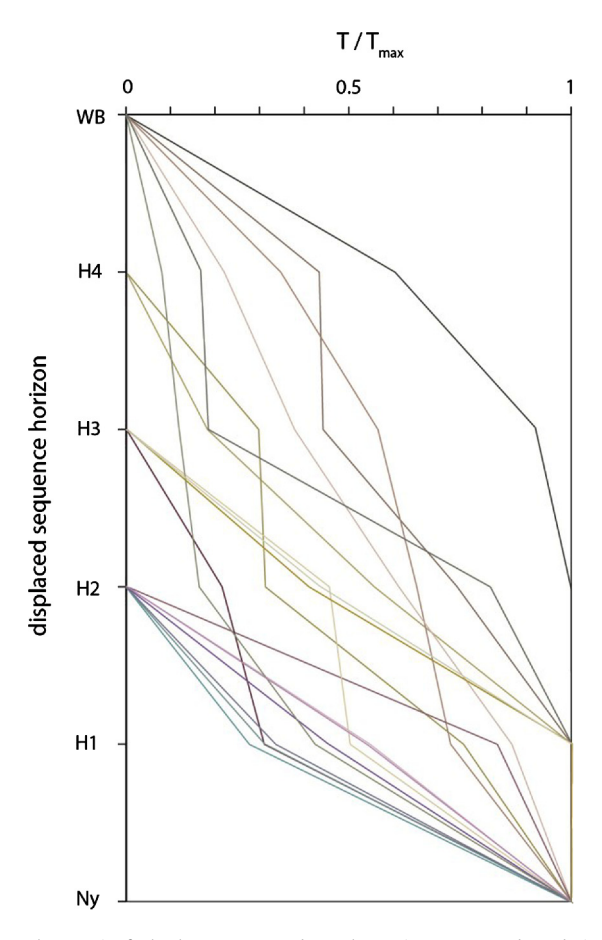


Fig. 9. Changes in fault throw measured on the major sequence boundaries for growth faults in the Kigoma basin. Lines connect throw values measured on major horizons. Isolated faults (20% of faults measured) were not included, as the timing of the initiation cannot be assessed from such an analysis. Measurements collected from seismic profile line ION-PROBE 84-210. The different sequence boundaries and an interpreted section are presented in Fig. 3. All throw data are normalized by dividing throw (T) by maximum throw (T_{max}). The deepest horizons occur at the base of the graph (i.e., Ny) and shallowest at the top (WB), thus these data illustrate changes in fault throw up the syn-rift sequence. For growth faults, maximum throw is observed on the acoustic basement horizon and decreases to zero by the surface horizon (WB). Periods of fault activity can be inferred by observing where fault throw decreases between sequence horizons.

fault trends (see also Corti et al. (2013) for examples from the Main Ethiopian Rift). However, local stress rotations in south Lake Tanganyika may also be driven by the broad NE–SW orientation of local Precambrian terranes (Daly et al., 1989), as the maximum horizontal stress can theoretically reorient and align parallel to relatively weak, lithospheric discontinuities (Morley, 2010).

5.2. Fault system evolution in the Lake Tanganyika Rift

Our analysis of fault system development in the Kigoma basin and Lake Tanganyika Rift generally, provides important insights into rift evolution in magma-poor regions of the EARS. The pre-existing basement fabric and recent rift faults are roughly parallel (Fig. 7), suggesting that inherited structures in part played a role in localizing fault strain. Although some authors advocate fault reactivation under oblique-dextral-slip in this part of the rift (Klerkx et al., 1998, and references therein), most faults in Lake Tanganyika strike orthogonal to the present day least compressive stress direction of Delvaux and Barth (2010). As such, we suggest that inherited basement weaknesses were reactivated as normal faults when optimally oriented to the principal stresses acting across the Lake Tanganyika Rift, resulting in the dominantly dip-slip behavior recorded during recent earthquake events (Delvaux and Barth,

Table 1Fault throws along major sequence boundaries for all growth faults in the Kigoma Basin on seismic line ION-PROBE 84-210 (horizons presented in Fig. 3). The cumulative throw for each sequence boundary is presented as well as the total throw accumulated during the deposition of the sequence directly overlying each boundary (seq. throw). All faults are presented in Fig. 3.

Fault no.	Fault throw (m) on sequence boundary					
	Ny	H1	H2	Н3	H4	WB
1	228.6	123	0	0	0	0
2	55.65	0	0	0	0	0
4	32.2	14.6	0	0	0	0
6	106.1	77.3	69.2	60	36.9	0
7	973.6	413.3	159.8	115.5	78.4	0
8	32.2	32.2	14	0	0	0
9	52.8	40	16.5	15.7	0	0
11	35.6	35.6	35.6	32.8	21.4	0
12	28.5	0	0	0	0	0
13	109.9	30.4	0	0	0	0
14	161.2	161.2	119.8	71.3	69.9	0
15	132.7	72.7	0	0	0	0
16	41.4	41.4	0	0	0	0
17	63.6	32	29	0	0	0
19	6	5	0	0	0	0
20	119	40	0	0	0	0
21	209	181	128	79	46	0
22	60	19	0	0	0	0
23	170	170	139	31	0	0
24	65	65	0	0	0	0
25	20	20	0	0	0	0
26	287	287	160	53	48	0
27	28	28	0	0	0	0
30	116	36	25	0	0	0
31	46	46	19	0	0	0
cum. throw (m)	3180.05	1970.7	914.9	458.3	300.6	0
seq. throw (m)	1209.35	1055.8	456.6	157.7	300.6	0

2010). As most faults strike normal to the present-day least compressive stress, and in some provinces do not parallel the inherited basement fabric (e.g., Ruzizi Province; Fig. 7A), the presence of these pre-existing lineaments is not considered here to have played the primary role in controlling strain localization into the Lake Tanganyika region.

Extension across the Lake Tanganyika region (~11.5 km for a β -factor of 1.283) was primarily accommodated along border fault structures over the lifetime of rifting, where in the Kigoma basin border faults account for ~ 10 km of heave and $\sim 87\%$ of the total extensional strain. Syn-depositional fault analyses reveal that the intra-rift fault system established early in the basin history. These intra-rift faults were more active during deposition of the two lowermost sequences (Sequences 1-2), when 60-70% of the total strain recorded in the intra-rift fault population was accommodated. The reduction in total throw observed in Plio-Pleistocene sequences (S3–5) suggests that activity in the intra-rift fault population diminished during this time. Unit expansion towards border faults is observed in all syn-rift sequences, and suggests continuous border fault activity throughout the basin's history. However, isopach thickness maps for syn-rift sequences (Rosendahl et al., 1988) are consistent with greater unit expansion towards border faults in Sequences 3-5, suggesting greater border fault activity during the later rift stages. The cumulative border fault throw (~13 km) observed along ION-PROBE line 84-210 in Lake Tanganyika is greater than typical estimates for early-stage rifts in the Eastern branch (e.g., up to 5 km of border fault throw; Muirhead et al., 2016), excluding the \sim 7 km-deep south Lokichar basin of the broadly rifted, \sim 25–30 Ma Lake Turkana Rift (Morley et al., 1992). However, it is comparable to the large offsets on other border faults in the Western branch (e.g., Accardo et al., 2018; Contreras et al., 2000). Overall, these results suggest longer-lived border fault activity in developing rift basins in the Western branch compared to those in Eastern branch (see also Accardo et al., 2018), and potentially increasing rates of border fault slip even as basins develop within the first 10 Myr of rifting.

5.3. Rift evolution in the absence of voluminous magmatism in the EARS

We see no evidence for a transition from border fault- to intra-rift fault-dominated strain accommodation along the rift axis within the first 10 Myr of rifting in the Lake Tanganyika Rift. This observation contrasts with those in evolving rift systems in the magma-rich Eastern branch (Hayward and Ebinger, 1996; Corti, 2009; Muirhead et al., 2016) (Fig. 10). The transition to intrarift dominated strain accommodation represents a critical step in conceptual rift models for the EARS as they evolve toward complete continental rupture (Ebinger, 2005; Corti, 2008, 2009). Indeed, many models and observations illustrate that nascent seafloor spreading segments are established below these fault systems along the rift axis (Corti, 2009; Ebinger and Casey, 2001; Keir et al., 2006; Muirhead et al., 2016; Wright et al., 2012). Observations of active early-stage rifting in the Eastern branch reveal that strain focusing to the rift center coincides with, and is probably assisted by, large magma and magmatic volatile fluxes in the mid- to lower crust in the rift center (Lee et al., 2016; Muirhead et al., 2016; Weinstein et al., 2017). This strain focusing occurs within the first 7 million years of rifting in Kenyan and Tanzanian sectors of the EARS (Muirhead et al., 2016) (Fig. 10).

The extensional forces required to rift lithosphere via magmatic diking are less than those required for normal faulting, and thus it is theoretically challenging to break apart initially strong continental lithosphere in the absence of magma (i.e., Buck, 2004; Bialas et al., 2010). Seismic reflection observations of magma-poor margins in the North and Central Atlantic (Reston, 2009), combined with field and numerical modeling results (Lavier and Manatschal, 2006), provide insights into the processes driving complete continental rupture in the absence of magma. Of these, the Iberian-Newfoundland margin represents a type example of a magmapoor rifted margin (Whitmarsh et al., 2001; Manatschal, 2004; Shillington et al., 2006; Peron-Pinvidic and Manatschal, 2009; Peron-Pinvidic et al., 2013). This margin had an initial crust composed of a ~24 km-thick quartz-feldspathic layer underlain by a ~6 km-thick gabbroic layer, resulting in a ductile middle crust overlying a stronger lower crustal section (Müntener et al., 2000; Manatschal, 2004; Peron-Pinvidic and Manatschal, 2009; Reston, 2009). During the initial stretching phase (e.g., Peron-Pinvidic et al., 2013), normal faults typically occur as low-angle listric faults that are rooted in a weak, ductile middle crust (Manatschal and Bernoulli, 1999; Whitmarsh et al., 2001; Lavier and Manatschal, 2006). Numerical modeling results suggest that ductile flow in a weak middle crust over the strong mafic lower crust allows for delocalization of upper and lower crustal deformation; this mechanical decoupling and development of ductile shear zones in the middle crust are considered essential for the magma-poor rifting model of Lavier and Manatschal (2006) (see also Mohn et al., 2012).

The Lake Tanganyika Rift and Western branch exhibit initial rift conditions that contrast with those for successfully rifted magmapoor margins (e.g., North and Central Atlantic margins; Reston, 2009). Restored cross-sections balance with straight, planar faults rather than listric normal faults (Fig. 8). Depth to detachment calculations indicate faults penetrate the entire seismogenic layer (Morley, 1988), with the depth-distribution of seismicity supporting border faulting to lower crustal depths (up to 34 km in \sim 42 km-thick crust; Nyblade and Langston, 1995; Camelbeeck and Iranga, 1996) rather than merging into mid-crustal detachments. Similarly, the length-scale of observed border faults necessitates a thick elastic layer (>25 km; Ebinger et al., 1999). These ob-

A Western rift branch B Eastern rift branch (Magadi & Natron basins) (Tanganyika & Malawi basins) border fault axial strain train accommodation accommodation active dike/sill intrusion minor lower mid- to lower crustal magmatism crustal melt mafic lower crust (cooled intrusions) upper mantle melt Tanganyika-Malawi Natron-Magadi rift basins rift basins age ~6-10 Ma1-2 ~3-7 Ma⁶⁻⁷ initial crustal thickness 41-42 km³ 37-40 km⁸⁻⁹ beta factor 1.28 - 1.33 3,19 1.36-1.488-9 max, border fault throw ~13 km^{19,*} ~5 km¹⁰ max. syn-rift fill thickness 5 km¹⁹ 3.5 km^{9,11} no¹⁹ yes^{9,12-14} upper crustal intrusions yes^{9,15} lower crustal magmatism yes, minor³ $n0^{4-5}$ ves^{12,16} mafic lower crust yes¹⁷⁻¹⁸ $n0^{3-5}$ upper mantle melting

Fig. 10. Simplified conceptual illustration of the basin architecture of early-stage rifts (<10 Ma) in both the (a) Western and (b) Eastern branches of the EARS. A & B) Conceptual models for early-stage rifts based on existing geological, geochemical, and geophysical data for the (a) Tanganyika and Malawi basins, and (b) Natron and Magadi basins. (c) Table broadly summarizing key aspects of the crustal and upper mantle architecture, and tectonic-magmatic attributes of each sector of the rift presented in (a) and (b). Although minor amounts of lower crustal magmatism have been inferred along rift axes for some Western branch basins (Hodgson et al., 2017), no upper mantle melt sources have been detected below the axes of any rifts, and lower crustal magmas may instead be sourced from the asthenosphere. References presented as superscript numbers in the main table: (1) Ebinger et al. (1993); (2) Cohen et al. (1993); Hodgson et al. (2017); (4) O'Donnell et al. (2015); (5) Accardo et al. (2017); (6) Crossley (1979); (7) Foster et al. (1997); (8) Mechie et al. (1994); (9) Weinstein et al. (2017); (10) Muirhead et al. (2016); (11) Birt et al. (1997); (12) Ibs-von Seht et al. (2001); (13) Calais et al. (2008); (14) Biggs et al. (2009); (15) Roecker et al. (2017); (16) Baker et al. (1971); (17) Mana et al. (2015); (18) Plasman et al. (2017); (19) this study.

servations support a thick, strong crust and lithosphere in the EARS (Chesley et al., 1999; Vauchez et al., 2005), which is theoretically too strong to break apart with the currently available tectonic forces (e.g., gravitation potential energy, basal shear from mantle convection; Coblentz and Sandiford, 1994; Bird et al., 2008; Stamps et al., 2015).

If the initial rift conditions documented for archetypal magmapoor margins (e.g., Iberian–Newfoundland margin; Peron-Pinvidic et al., 2013) are necessary precursors to successful continental breakup, then complete continental rupture in the Western branch currently seems unlikely. Our analysis, however, does not necessarily preclude later development of detachment faults and mid-crustal decoupling layers that could assist future break up (Rosenbaum et al., 2010). Future lithospheric thinning and related decompression melting may also drive the generation of sufficient magma volumes below the Lake Tanganyika Rift, thus transitioning the system towards a more magmatic mode of extension and

rift evolution (e.g., Ebinger, 2005). Nonetheless, in the absence of voluminous magmatism, we suggest that either (1) complete continental rupture cannot be achieved in the Western branch of the EARS, or (2) continental break up in the Western branch will proceed under a model that contrasts with that invoked for both the Eastern branch and magma-poor rifted margins generally.

6. Conclusions

We investigated a \sim 10 million-year history of faulting in the Lake Tanganyika Rift, to document how fault systems evolve in the magma-poor Western branch of the EARS. Reprocessed legacy and high-resolution commercial seismic reflection datasets provide a revised structural framework for this multi-segment rift. Syn-depositional fault analyses and structural reconstructions of the Kigoma basin reveal how fault throw and extensional strain were distributed during different depositional sequences. Unlike

^{*}Total accumulated throw on both the western and eastern border faults of the Kigoma basin.

the magma-rich Eastern branch, fault-strain has not focused along the basin floor along the rift axis within the first $\sim \! 10$ million years of rifting. Instead, large border faults continue to accommodate the majority of extension. These observations point to contrasting fault behavior in the Western and Eastern branches, potentially related to the absence of significant magma volumes in the Western branch. Existing models for successful rift evolution in the EARS suggest that the transition to axial rifting represents a critical step in the evolution toward sea-floor spreading. Furthermore, the Western branch exhibits initial rift conditions that contrast with those of successfully rifted magma-poor margins. In the absence of voluminous magmatism, if complete continental rupture were achieved in the Western branch of the EARS it would proceed under a model that contrasts with that invoked for the Eastern branch and magma-poor rifted margins generally.

Acknowledgements

Reflection seismic data used in this study were reprocessed by ION Geophysical, and were acquired in 1983-1984 by Project PROBE of Duke University, under the direction of B.R. Rosendahl. Analyses of the reprocessed data were performed with the support of industry partners Africa Energy, Chevron, Maersk Oil (now Total), and RakGas. Additional high-resolution multi-channel seismic data were provided with the support of the Tanzanian Petroleum Development Corporation and Beach Energy Ltd. JDM and CAS acknowledge the support of National Science Foundation Grant EAR-1654518. DecisionSpace software licenses were provided by Landmark-Haliburton. ASTER GDEM is a product of NASA and METI. We gratefully acknowledge the assistance of members of the Lacustrine Basin Research Group, particularly Peter Cattaneo, Jacqueline Corbett, and Mattie Friday, as well as Emily Judd. Jeff Karson and Donna Shillington kindly provided paper comments prior to submission. We thank reviewers Derek Keir and an anonymous reviewer for detailed and constructive comments that greatly improved the manuscript, and Jean-Phillip Avouac for editorial handling.

Appendix A. Supplementary material

Supplementary material related to this article can be found online at https://doi.org/10.1016/j.epsl.2018.11.004.

References

- Accardo, N.J., Gaherty, J.B., Shillington, D.J., Ebinger, C.J., Nyblade, A.A., Mbogoni, G.J., Chindandali, P.R.N., Ferdinand, R.W., Mulibo, G.D., Kamihanda, G., Keir, D., Scholz, C.A., Selway, K., O'Donnell, J.P., Tepp, G., Gallacher, R.J., Mtelela, K., Salima, J., Mruma, A., 2017. Surface wave imaging of the weakly extended Malawi Rift from ambient-noise and teleseismic Rayleigh waves from onshore and lakebottom seismometers. Geophys. J. Int. 209, 1892–1905. https://doi.org/10.1093/gji/ggx133.
- Accardo, N.J., Shillington, D.J., Gaherty, J.B., Scholz, C.A., Ebinger, C.J., Nyblade, A.A., Chindandali, P.R.N., Kamihanda, G., McCartney, T., Wood, D., 2018. Constraints on rift basin structure and border fault growth in the northern Malawi rift from 3D seismic refraction imaging. J. Geophys. Res., Solid Earth. https://doi.org/10.1029/2018/B016504.
- Agostini, A., Corti, G., Zeoli, A., Mulugeta, G., 2009. Evolution, pattern, and partitioning of deformation during oblique continental rifting: inferences from lithospheric-scale centrifuge models. Geochem. Geophys. Geosyst. 10. https://doi.org/10.1029/2009gc002676.
- Agostini, A., Bonini, M., Corti, G., Sani, F., Manetti, P., 2011. Distribution of quaternary deformation in the central Main Ethiopian Rift, East Africa. Tectonics 30. https://doi.org/10.1029/2010tc002833.
- Baker, B.H., Williams, L.A., Miller, J.A., Fitch, F.J., 1971. Sequence and geochronology of Kenya Rift volcanics. Tectonophysics 11, 191–215. https://doi.org/10.1016/0040-1951(71)90030-8.
- Baudon, C., Cartwright, J., 2008. Early stage evolution of growth faults: 3D seismic insights from the Levant Basin, Eastern Mediterranean. J. Struct. Geol. 30, 888–898. https://doi.org/10.1016/j.jsg.2008.02.019.

- Berryman, K., Villamor, P., Nairn, I., van Dissen, R., Begg, J., Lee, J., 2008. Late Pleistocene surface rupture history of the Paeroa Fault, Taupo Rift, New Zealand. N.Z. J. Geol. Geophys. 51, 135–158. https://doi.org/10.1080/00288300809509855.
- Beutel, E., van Wijk, J., Ebinger, C., Keir, D., Agostini, A., 2010. Formation and stability of magmatic segments in the Main Ethiopian and Afar rifts. Earth Planet. Sci. Lett. 293, 225–235. https://doi.org/10.1016/j.epsl.2010.02.006.
- Bialas, R.W., Buck, W.R., Qin, R., 2010. How much magma is required to rift a continent? Earth Planet. Sci. Lett. 292, 68–78. https://doi.org/10.1016/j.epsl.2010.01.
- Biggs, J., Anthony, E.Y., Ebinger, C.J., 2009. Multiple inflation and deflation events at Kenyan volcanoes, East African Rift. Geology 37, 979–982. https://doi.org/10.1130/g30133a.1.
- Biggs, J., Nissen, E., Craig, T., Jackson, J., Robinson, D.P., 2010. Breaking up the hanging wall of a rift-border fault: the 2009 Karonga earthquakes, Malawi. Geophys. Res. Lett. 37. https://doi.org/10.1029/2010GL043179.
- Biggs, J., Bastow, I.D., Keir, D., Lewi, E., 2011. Pulses of deformation reveal frequently recurring shallow magmatic activity beneath the Main Ethiopian Rift. Geochem. Geophys. Geosyst. 12. https://doi.org/10.1029/2011gc003662.
- Bird, P., Liu, Z., Rucker, W.K., 2008. Stresses that drive the plates from below: definitions, computational path, model optimization, and error analysis. J. Geophys. Res., Solid Earth 113. https://doi.org/10.1029/2007jb005460.
- Birt, C.S., Maguire, P.K.H., Khan, M.A., Thybo, H., Keller, G.R., Patel, J., 1997. The influence of pre-existing structures on the evolution of the southern Kenya Rift Valley—evidence from seismic and gravity studies. Tectonophysics 278, 211–242.
- Botz, R.W., Stoffers, P., 1993. Light hydrocarbon gases in Lake Tanganyika hydrothermal fluids (east-central Africa). Chem. Geol. 104, 217–224. https://doi.org/10.1016/0009-2541(93)90152-9.
- Buck, W.R., 2004. Consequences of asthenospheric variability on continental rifting. In: Rheology and Deformation of the Lithosphere at Continental Margins, pp. 1–30.
- Calais, E., d'Oreye, N., Albaric, J., Deschamps, A., Delvaux, D., Deverchere, J., Ebinger, C., Ferdinand, R.W., Kervyn, F., Macheyeki, A.S., Oyen, A., Perrot, J., Saria, E., Smets, B., Stamps, D.S., Wauthier, C., 2008. Strain accommodation by slow slip and dyking in a youthful continental rift, East Africa. Nature 456, 783–788. https://doi.org/10.1038/nature07478.
- Camelbeeck, T., Iranga, M.D., 1996. Deep crustal earthquakes and active faults along the Rukwa trough, Eastern Africa. Geophys. J. Int. 124, 612–630. https://doi.org/10.1111/j.1365-246X.1996.tb07040.x.
- Cartwright, J., Bouroullec, R., James, D., Johnson, H., 1998. Polycyclic motion history of some Gulf Coast growth faults from high-resolution displacement analysis. Geology 26, 819–822. https://doi.org/10.1130/0091-7613(1998)026<0819: PMHOSG>2.3.CO:2.
- Chesley, J.T., Rudnick, R.L., Lee, C.T., 1999. Re–Os systematics of mantle xenoliths from the East African Rift: age, structure, and history of the Tanzanian craton. Geochim. Cosmochim. Acta 63, 1203–1217. https://doi.org/10.1016/s0016-7037(99)00004-6.
- Choubert, G., Faure-Muret, A., 1968. International tectonic map of Africa. ASGA map, scale 1:5 000 000, 9 sheets.
- Coblentz, D.D., Sandiford, M., 1994. Tectonic stresses in the African plate: constraints on the ambient lithospheric stress state. Geology 22, 831–834. https://doi.org/10.1130/0091-7613(1994)022<0831:tsitap>2.3.co;2.
- Cohen, A.S., Soreghan, M.J., Scholz, C.A., 1993. Estimating the age of formation of lakes an example from Lake Tanganyika, East African Rift System. Geology 21, 511–514. https://doi.org/10.1130/0091-7613(1993)021<0511:etaofo>2.3.co;2.
- Contreras, J., Anders, M.H., Scholz, C.H., 2000. Growth of a normal fault system: observations from the Lake Malawi basin of the east African rift. J. Struct. Geol. 22, 159–168. https://doi.org/10.1016/s0191-8141(99)00157-1.
- Corti, G., 2008. Control of rift obliquity on the evolution and segmentation of the main Ethiopian rift. Nat. Geosci. 1, 258–262. https://doi.org/10.1038/ngeo160.
- Corti, G., 2009. Continental rift evolution: from rift initiation to incipient break-up in the Main Ethiopian Rift, East Africa. Earth-Sci. Rev. 96, 1–53. https://doi.org/ 10.1016/j.earscirev.2009.06.005.
- Corti, G., Bonini, M., Sokoutis, D., Innocenti, F., Manetti, P., Cloetingh, S., Mulugeta, G., 2004. Continental rift architecture and patterns of magma migration: a dynamic analysis based on centrifuge models. Tectonics 23, 1–20. https://doi.org/10.1029/ 2003tc001561.
- Corti, G., Philippon, M., Sani, F., Keir, D., Kidane, T., 2013. Re-orientation of the extension direction and pure extensional faulting at oblique rift margins: comparison between the Main Ethiopian Rift and laboratory experiments. Terra Nova 25, 396–404. https://doi.org/10.1111/ter.12049.
- Crossley, R., 1979. The Cenozoic stratigraphy and structure of the western part of the rift valley in southern Kenya. J. Geol. Soc. 136, 393–405.
- Daly, M.C., Chorowicz, J., Fairhead, J.D., 1989. Rift basin evolution in Africa: the influence of steep basement shear zones. Geol. Soc. (Lond.) Spec. Publ. 44, 309–334.
- Delvaux, D., Barth, A., 2010. African stress pattern from formal inversion of focal mechanism data. Tectonophysics 482, 105–128. https://doi.org/10.1016/j.tecto. 2009.05.009.
- Duffy, O.B., Bell, R.E., Jackson, C.A.L., Gawthorpe, R.L., Whipp, P.S., 2015. Fault growth and interactions in a multiphase rift fault network: Horda Platform, Norwegian North Sea. J. Struct. Geol. 80, 99–119. https://doi.org/10.1016/j.jsg.2015.08.015.

- Dunkelman, T.J., Rosendahl, B.R., Karson, J.A., 1989. Structure and stratigraphy of the Turkana rift from seismic reflection data. J. Afr. Earth Sci. 8, 489–510. https:// doi.org/10.1016/S0899-5362(89)80041-7.
- Ebinger, C., 2005. Continental break-up: the East African perspective. Astron. Geophys. 46. 16-21.
- Ebinger, C.J., Casey, M., 2001. Continental breakup in magmatic provinces: an Ethiopian example. Geology 29, 527–530. https://doi.org/10.1130/0091-7613(2001)029<0527:cbimpa>2.0.co;2.
- Ebinger, C., Scholz, C.A., 2012. Continental rift basins: the East African perspective. In: Tectonics of Sedimentary Basins: Recent Advances, pp. 185–208.
- Ebinger, C.J., Karner, G.D., Weissel, J.K., 1991. Mechanical strength of extended continental lithosphere: constraints from the Western rift system, East Africa. Tectonics 10, 1239–1256. https://doi.org/10.1029/91tc00579.
- Ebinger, C.J., Deino, A.L., Tesha, A.L., Becker, T., Ring, U., 1993. Tectonic controls on rift basin morphology: evolution of the Northern Malawi (Nyasa) Rift. J. Geophys. Res., Solid Earth 98, 17821–17836.
- Ebinger, C.J., Jackson, J.A., Foster, A.N., Hayward, N.J., 1999. Extensional basin geometry and the elastic lithosphere. Philos. Trans. R. Soc. Lond. Ser. A Math. Phys. Eng. Sci. 357, 741–762. https://doi.org/10.1098/rsta.1999.0351.
- Foster, A., Ebinger, C., Mbede, E., Rex, D., 1997. Tectonic development of the northern Tanzanian sector of the East African Rift System. J. Geol. Soc. 154, 689–700.
- Franke, D., 2013. Rifting, lithosphere breakup and volcanism: comparison of magma-poor and volcanic rifted margins. Mar. Pet. Geol. 43, 63–87. https://doi.org/10.1016/j.marpetgeo.2012.11.003.
- Hayward, N.J., Ebinger, C.J., 1996. Variations in the along-axis segmentation of the Afar Rift system. Tectonics 15, 244–257. https://doi.org/10.1029/95tc02292.
- Hodgson, I., Illsley-Kemp, F., Gallacher, R.J., Keir, D., Ebinger, C.J., Mtelela, K., 2017. Crustal structure at a young continental rift: a receiver function study from the Tanganyika Rift. Tectonics 36, 2806–2822. https://doi.org/10.1002/ 2017TC004477.
- Hunt, J.A., Zafu, A., Mather, T.A., Pyle, D.M., Barry, P.H., 2017. Spatially variable CO₂ degassing in the Main Ethiopian Rift: implications for magma storage, volatile transport, and rift-related emissions. Geochem. Geophys. Geosyst. 18, 3714–3737. https://doi.org/10.1002/2017GC006975.
- Ibs-von Seht, M., Blumenstein, S., Wagner, R., Hollnack, D., Wohlenberg, J., 2001. Seismicity, seismotectonics and crustal structure of the southern Kenya Rift-new data from the Lake Magadi area. Geophys. J. Int. 146, 439–453.
- Jackson, C.A.L., Rotevatn, A., 2013. 3D seismic analysis of the structure and evolution of a salt-influenced normal fault zone: a test of competing fault growth models. J. Struct. Geol. 54, 215–234. https://doi.org/10.1016/j.jsg.2013.06.012.
- Karson, J.A., Curtis, P.C., 1989. Tectonic and magmatic processes in the eastern branch of the East African rift and implications for magmatically active continental rifts. J. Afr. Earth Sci. 8, 431–453. https://doi.org/10.1016/S0899-5362(89) 80037-5.
- Keir, D., Ebinger, C.J., Stuart, G.W., Daly, E., Ayele, A., 2006. Strain accommodation by magmatism and faulting as rifting proceeds to breakup: seismicity of the northern Ethiopian rift. J. Geophys. Res., Solid Earth 111. https://doi.org/10.1029/ 2005jb003748.
- Keir, D., Bastow, I.D., Whaler, K.A., Daly, E., Cornwell, D.G., Hautot, S., 2009. Lower crustal earthquakes near the Ethiopian rift induced by magmatic processes. Geochem. Geophys. Geosyst. 10. https://doi.org/10.1029/2009gc002382.
- Kilembe, E.A., Rosendahl, B.R., 1992. Structure and stratigraphy of the Rukwa Rift. Tectonophysics 209, 143–158. https://doi.org/10.1016/0040-1951(92)90016-y.
- Klerkx, J., Theunissen, K., Delvaux, D., 1998. Persistent fault controlled basin formation since the Proterozoic along the Western Branch of the East African Rift. J. Afr. Earth Sci. 26, 347–361. https://doi.org/10.1016/s0899-5362(98)00020-7.
- Kolawole, F., Atekwana, E.A., Malloy, S., Stamps, D.S., Grandin, R., Abdelsalam, M.G., Leseane, K., Shemang, E.M., 2017. Aeromagnetic, gravity, and Differential Interferometric Synthetic Aperture Radar analyses reveal the causative fault of the 3 April 2017 Mw 6.5 Moiyabana, Botswana, earthquake. Geophys. Res. Lett. 44, 8837–8846. https://doi.org/10.1002/2017GL074620.
- Lavier, L.L., Manatschal, G., 2006. A mechanism to thin the continental lithosphere at magma-poor margins. Nature 440, 324–328. https://doi.org/10.1038/nature04608.
- Lee, H., Muirhead, J.D., Fischer, T.P., Ebinger, C.J., Kattenhorn, S.A., Sharp, Z.D., Kianji, G., 2016. Massive and prolonged deep carbon emissions associated with continental rifting. Nat. Geosci. https://doi.org/10.1038/NGE02622.
- Lee, H., Fischer, T.P., Muirhead, J.D., Ebinger, C.J., Kattenhorn, S.A., Sharp, Z.D., Kianji, G., Takahataf, N., Sano, Y., 2017. Incipient rifting accompanied by the release of subcontinental lithospheric mantle volatiles in the Magadi and Natron basin, East Africa. J. Volcanol. Geotherm. Res. 346, 118–133. https://doi.org/10.1016/j.jvolgeores.2017.03.017.
- Macgregor, D., 2015. History of the development of the East African Rift System: a series of interpreted maps through time. J. Afr. Earth Sci. 101, 232–252. https:// doi.org/10.1016/j.jafrearsci.2014.09.016.
- Mana, S., Furman, T., Turrin, B.D., Feigenson, M.D., Swisher III, C.C., 2015. Magmatic activity across the East African North Tanzanian Divergence Zone. J. Geol. Soc. 172, 368–389. https://doi.org/10.1144/jgs2014-072.
- Manatschal, G., 2004. New models for evolution of magma-poor rifted margins based on a review of data and concepts from West Iberia and the Alps. Int. J. Earth Sci. 93, 432–466. https://doi.org/10.1007/s00531-004-0394-7.

- Manatschal, G., Bernoulli, D., 1999. Architecture and tectonic evolution of nonvolcanic margins: present-day Galicia and ancient Adria. Tectonics 18, 1099–1119. https://doi.org/10.1029/1999tc900041.
- McCartney, T., Scholz, C.A., 2016. A 1.3 million year record of synchronous faulting in the hangingwall and border fault of a half-graben in the Malawi (Nyasa) Rift. J. Struct. Geol. 91, 114–129. https://doi.org/10.1016/j.jsg.2016.08.012.
- Mechie, J., Keller, G.R., Prodehl, C., Gaciri, S., Braile, L.W., Mooney, W.D., Gajewskif, D., Sandmeier, K.J., 1994. Crustal structure beneath the Kenya Rift from axial profile data. Tectonophysics 236, 179–200. https://doi.org/10.1016/0040-1951(94) 90176-7
- Mohn, G., Manatschal, G., Beltrando, M., Masini, E., Kusznir, N., 2012. Necking of continental crust in magma-poor rifted margins: evidence from the fossil Alpine Tethys margins. Tectonics 31. https://doi.org/10.1029/2011tc002961.
- Mohr, P.A., Wood, C.A., 1976. Volcano spacings and lithospheric attenuation in the Eastern Rift of Africa. Earth Planet. Sci. Lett. 33, 126–144. https://doi.org/10. 1016/0012-821X(76)90166-7.
- Morley, C.K., 1988. Variable extension in Lake Tanganyika. Tectonics 7, 785–801. https://doi.org/10.1029/TC007i004p00785.
- Morley, C.K., Wescott, W.A., Stone, D.M., Harper, R.M., Wigger, S.T., Karanja, F.M., 1992. Tectonic evolution of the northern Kenya Rift. J. Geol. Soc. 149, 333–348. https://doi.org/10.1144/gsjgs.149.3.0333.
- Morley, C.K., 2010. Stress re-orientation along zones of weak fabrics in rifts: an explanation for pure extension in 'oblique' rift segments? Earth Planet. Sci. Lett. 297, 667–673. https://doi.org/10.1016/j.epsl.2010.07.022.
- Muirhead, J.D., Kattenhorn, S.A., 2018. Activation of preexisting transverse structures in an evolving magmatic rift in East Africa. J. Struct. Geol. 106, 1–18. https://doi.org/10.1016/j.jsg.2017.11.004.
- Muirhead, J.D., Kattenhorn, S.A., Le Corvec, N., 2015. Varying styles of magmatic strain accommodation in the East African Rift. Geochem. Geophys. Geosyst. 16. https://doi.org/10.1002/2015gc005918.
- Muirhead, J.D., Kattenhorn, S.A., Lee, H., Mana, S., Turrin, B.D., Fischer, T.P., Kianji, G., Dindi, E., Stamps, D.S., 2016. Evolution of upper crustal faulting assisted by magmatic volatile release during early-stage continental rift development in the East African Rift. Geosphere 12, 1670–1700. https://doi.org/10.1130/ges01375.1.
- Muntener, O., Hermann, J., Trommsdorff, V., 2000. Cooling history and exhumation of lower crustal granulite and Upper Mantle (Malenco, Eastern Central Alps). J. Petrol. 41, 175–200. https://doi.org/10.1093/petrology/41.2.175.
- Nyblade, A.A., Langston, C.A., 1995. East African earthquakes below 20 km depth and implications for crustal structure. Geophys. J. Int. 121, 49–62. https://doi. org/10.1111/j.1365-246X.1995.tb03510.x.
- O'Donnell, J.P., Adams, A., Nyblade, A.A., Mulibo, G.D., Tugume, F., 2013. The uppermost mantle shear wave velocity structure of eastern Africa from Rayleigh wave tomography: constraints on rift evolution. Geophys. J. Int. 194, 961–978. https://doi.org/10.1093/gji/ggt135.
- O'Donnell, J.P., Selway, K., Nyblade, A.A., Brazier, R.A., Tahir, N.E., Durrheim, R.J., 2015. Thick lithosphere, deep crustal earthquakes and no melt: a triple challenge to understanding extension in the western branch of the East African Rift. Geophys. J. Int. 204, 985–998. https://doi.org/10.1093/gji/ggv492.
- Peron-Pinvidic, G., Manatschal, G., 2009. The final rifting evolution at deep magmapoor passive margins from Iberia-Newfoundland: a new point of view. Int. J. Earth Sci. 98, 1581–1597. https://doi.org/10.1007/s00531-008-0337-9.
- Peron-Pinvidic, G., Manatschal, G., Osmundsen, P.T., 2013. Structural comparison of archetypal Atlantic rifted margins: a review of observations and concepts. Mar. Pet. Geol. 43, 21–47. https://doi.org/10.1016/j.marpetgeo.2013.02.002.
- Plasman, M., Tiberi, C., Ebinger, C., Gautier, S., Albaric, J., Peyrat, S., Déverchère, J., Le Gall, B., Tarits, P., Roecker, S., Wambura, F., Muzuka, A., Mulibo, G., Mtelela, K., Msabi, M., Kianji, G., Hautot, S., Perrot, J., Gama, J., 2017. Lithospheric low-velocity zones associated with a magmatic segment of the Tanzanian Rift, East Africa. Geophys. J. Int. 210, 465–481. https://doi.org/10.1093/gji/ggx177.
- Reston, T.J., 2009. The structure, evolution and symmetry of the magma-poor rifted margins of the North and Central Atlantic: a synthesis. Tectonophysics 468, 6–27. https://doi.org/10.1016/j.tecto.2008.09.002.
- Roberts, E.M., Stevens, N.J., O'Connor, P.M., Dirks, P.H.G.M., Gottfried, M.D., Clyde, W.C., Armstrong, R.A., Kemp, A.I.S., Hemming, S., 2012. Initiation of the western branch of the East African Rift coeval with the eastern branch. Nat. Geosci. 5, 289–294. https://doi.org/10.1038/ngeo1432.
- Roecker, S., Ebinger, C., Tiberi, C., Mulibo, G., Ferdinand-Wambura, R., Mtelela, K., Kianji, G., Muzuka, A., Gautier, S., Albaric, J., Peyrat, S., 2017. Subsurface images of the Eastern Rift, Africa, from the joint inversion of body waves, surface waves and gravity: investigating the role of fluids in early-stage continental rifting. Geophys. J. Int. 210, 931–950. https://doi.org/10.1093/gji/ggx220.
- Rosenbaum, G., Regenauer-Lieb, K., Weinberg, R.F., 2010. Interaction between mantle and crustal detachments: a nonlinear system controlling lithospheric extension. J. Geophys. Res., Solid Earth 115. https://doi.org/10.1029/2009jb006696.
- Rosendahl, B.R., 1987. Architecture of continental rifts with special reference to East Africa. Annu. Rev. Earth Planet. Sci. 15, 445–503. https://doi.org/10.1146/annurev.ea.15.050187.002305.
- Rosendahl, B.R., Scholz, C.A., Woods, L.D., 1988. Seismic Atlas of Lake Tanganyika. Project PROBE. Duke University. p. 81.

- Rosendahl, B.R., Kilembe, E., Kaczmarick, K., 1992. Comparison of the Tanganyika, Malawi, Rukwa and Turkana rift zones from analysis of seismic reflection data. Tectonophysics 213, 235–256. https://doi.org/10.1016/0040-1951(92)90261-4.
- Saria, E., Calais, E., Stamps, D.S., Delvaux, D., Hartnady, C.J.H., 2014. Present-day kinematics of the East African Rift. J. Geophys. Res., Solid Earth 119, 3584–3600. https://doi.org/10.1002/2013jb010901.
- Scholz, C.A., Rosendahl, B.R., 1988. Low lake stands in lakes Malawi and Tanganyika, East Africa, delineated with multifold seismic data. Science 240, 1645–1648. https://doi.org/10.1126/science.240.4859.1645.
- Scholz, C.A., Rosendahl, B.R., Scott, D.L., 1990. Development of coarse-grained facies in lacustrine rift basins: examples from East Africa. Geology 18, 140–144. https://doi.org/10.1130/0091-7613(1990)018<0140:docgfi>2.3.co;2.
- Scholz, C.A., King, J.W., Ellis, G.S., Swart, P.K., Stager, J.C., Colman, S.M., 2003. Paleolimnology of Lake Tanganyika, East Africa, over the past 100 k yr. J. Paleolimnol. 30, 139–150. https://doi.org/10.1023/a:1025522116249.
- Scholz, C.A., Johnson, T.C., Cohen, A.S., King, J.W., Peck, J.A., Overpeck, J.T., Talbot, M.R., Brown, E.T., Kalindekafe, L., Amoako, P.Y.O., Lyons, R.P., Shanahan, T.M., Castaneda, I.S., Heil, C.W., Forman, S.L., McHargue, L.R., Beuning, K.R., Gomez, J., Pierson, J., 2007. East African megadroughts between 135 and 75 thousand years ago and bearing on early-modern human origins. Proc. Natl. Acad. Sci. USA 104, 16416-16421. https://doi.org/10.1073/pnas.0703874104.
- Shillington, D.J., Holbrook, W.S., Van Avendonk, H.J.A., Tucholke, B.E., Hopper, J.R., Louden, K.E., Larsen, H.C., Nunes, G.T., 2006. Evidence for asymmetric non-volcanic rifting and slow incipient oceanic accretion from seismic reflection data on the Newfoundland margin. J. Geophys. Res., Solid Earth 111. https://doi.org/10.1029/2005jb003981.
- Shillington, D.J., Gaherty, J.B., Ebinger, C.J., Scholz, C.A., Selway, K., Nyblade, A.A., Bedrosian, P.A., Class, C., Nooner, S.L., Pritchard, M.E., Elliott, J., Chindandali, P.R.N., Mbogoni, G., Ferdinand, R.W., Boniface, N., Manya, S., Kamihanda, G., Saria, E., Mulibo, G., Salima, J., Mruma, A., Kalindekafe, L., Accardo, N.J., Ntambila, D., Kachingwe, M., Mesko, G.T., McCartney, T., Maquay, M., O'Donnell, J.P., Tepp, G., Mtelela, K., Trinhammer, P., Wood, D., Aaron, E., Gibaud, M., Rapa, M., Pfeifer, C., Mphepo, F., Gondwe, D., Arroyo, G., Eddy, C., Kamoga, B., Moshi, M., 2016. Acquisition of a unique onshore/offshore geophysical and geochemical dataset in the Northern Malawi (Nyasa) Rift. Seismol. Res. Lett. 87, 1406–1416. https://doi.org/10.1785/0220160112.
- Stab, M., Bellahsen, N., Pik, R., Quidelleur, X., Ayalew, D., Leroy, S., 2016. Modes of rifting in magma-rich settings: tectono-magmatic evolution of Central Afar. Tectonics 35, 2–38. https://doi.org/10.1002/2015TC003893.
- Stamps, D.S., Iaffaldano, G., Calais, E., 2015. Role of mantle flow in Nubia-Somalia plate divergence. Geophys. Res. Lett. 42, 290–296. https://doi.org/10. 1002/2014gl062515.

- Tiercelin, J.J., Soreghan, M., Cohen, A.S., Lezzar, K.E., Bouroullec, J.L., 1992. Sedimentation in large rift lakes: example from the Middle Pleistocene—Modern deposits of the Tanganyika Trough, East African Rift System. Bull. Cent. Rech. Explor. Prod. Elf-Aquitaine 16, 83–111.
- Vauchez, A., Dineur, F., Rudnick, R., 2005. Microstructure, texture and seismic anisotropy of the lithospheric mantle above a mantle plume: insights from the Labait volcano xenoliths (Tanzania). Earth Planet. Sci. Lett. 232, 295–314. https://doi.org/10.1016/j.epsl.2005.01.024.
- Versfelt, J., Rosendahl, B.R., 1989. Relationships between pre-rift structure and rift architecture in Lakes Tanganyika and Malawi, East Africa. Nature 337, 354–357. https://doi.org/10.1038/337354a0.
- Wauthier, C., Cayol, V., Poland, M., Kervyn, F., D'Oreye, N., Hooper, A., Samsonov, S., Tiampo, K., Smets, B., 2013. Nyamulagira's magma plumbing system inferred from 15 years of InSAR. In: Remote Sensing of Volcanoes and Volcanic Processes: Integrating Observation and Modelling. Geol. Soc. (Lond.) Spec. Publ. 380, 39–65. https://doi.org/10.1144/sp380.9.
- Wauthier, C., Smets, B., Keir, D., 2015. Diking-induced moderate-magnitude earth-quakes on a youthful rift border fault: the 2002 Nyiragongo-Kalehe sequence, DR Congo. Geochem. Geophys. Geosyst. 16, 4280–4291. https://doi.org/10.1002/2015gc006110.
- Weinstein, A., Oliva, S.J., Ebinger, C.J., Roecker, S., Tiberi, C., Aman, M., Lambert, C., Witkin, E., Albaric, J., Gautier, S., Peyrat, S., Muirhead, J.D., Muzuka, A.N.N., Mulibo, G., Kianji, G., 2017. Fault-magma interactions during early continental rifting: seismicity of the Magadi-Natron-Manyara basins, Africa. Geochem. Geophys. Geosyst. 18, 3662–3686. https://doi.org/10.1002/2017GC007027.
- Wheeler, W.H., Karson, J.A., 1994. Extension and subsidence adjacent to a weak continental transform: an example from the Rukwa Rift, East Africa. Geology 22, 625–628. https://doi.org/10.1130/0091-7613(1994)022<0625:easata>2.3.co;2.
- Whitmarsh, R.B., Manatschal, G., Minshull, T.A., 2001. Evolution of magma-poor continental margins from rifting to seafloor spreading. Nature 413, 150-154. https://doi.org/10.1038/35093085.
- Wright, T.J., Ebinger, C., Biggs, J., Ayele, A., Yirgu, G., Keir, D., Stork, A., 2006. Magmamaintained rift segmentation at continental rupture in the 2005 Afar dyking episode. Nature 442, 291–294. https://doi.org/10.1038/nature04978.
- Wright, T.J., Sigmundsson, F., Pagli, C., Belachew, M., Hamling, I.J., Brandsdottir, B., Keir, D., Pedersen, R., Ayele, A., Ebinger, C., Einarsson, P., Lewi, E., Calais, E., 2012. Geophysical constraints on the dynamics of spreading centres from rifting episodes on land. Nat. Geosci. 5, 242–250. https://doi.org/10.1038/ngeo1428.